MOLECULAR ECOLOGY

Molecular Ecology (2010) **19**, 146–169 doi: 10.1111/j.1365-294X.2009.04417.x

The 'Expansion–Contraction' model of Pleistocene biogeography: rocky shores suffer a sea change?

PETER B. MARKO,* JESSICA M. HOFFMAN,* SANDRA A. EMME,* TAMARA M. MCGOVERN,* CARSON C. KEEVER† and L. NICOLE COX*

**Department of Biological Sciences, Clemson University, Clemson, SC 29634-0314, USA, †Department of Biological Sciences, 8888 University Drive, Simon Fraser, University, Burnaby BC, V5A 1S6, Canada*

Abstract

Approximately 20 000 years ago the last glacial maximum (LGM) radically altered the distributions of many Northern Hemisphere terrestrial organisms. Fewer studies describing the biogeographic responses of marine species to the LGM have been conducted, but existing genetic data from coastal marine species indicate that fewer taxa show clear signatures of post-LGM recolonization. We have assembled a mitochondrial DNA (mtDNA) data set for 14 co-distributed northeastern Pacific rocky-shore species from four phyla by combining new sequences from ten species with previously published sequences from eight species. Nuclear sequences from four species were retrieved from GenBank, plus we gathered new elongation factor 1-α sequences from the barnacle *Balanus glandula*. Results from demographic analyses of mtDNA for five (36%) species (*Evasterias troschelii, Pisaster ochraceus, Littorina sitkana, L. scutulata, Xiphister mucosus*) were consistent with large population expansions occurring near the LGM, a pattern expected if these species recently recolonized the region. However, seven (50%) species (*Mytilus trossulus, M. californianus, B. glandula, S. cariosus, Patiria miniata, Katharina tunicata, X. atropurpureus*) exhibited histories consistent with long-term stability in effective population size, a pattern indicative of regional persistence during the LGM. Two species of *Nucella* with significant mtDNA genetic structure showed spatially variable demographic histories. Multilocus analyses for five species were largely consistent with mtDNA: the majority of multilocus interpopulation divergence times significantly exceeded the LGM. Our results indicate that the LGM did not extirpate the majority of species in the northeastern Pacific; instead, regional persistence during the LGM appears a common biogeographic history for rocky-shore organisms in this region.

Keywords: Bayesian demographic reconstruction, climate change, divergence times, marine invertebrates, mismatch analysis, mitochondria, population growth, post-glacial expansion, skyline plot

Received 30 June 2009; revision received 11 September 2009; accepted 28 September 2009

Introduction

Among the many factors affecting the abundance and distribution of species, climate change has by far received the greatest attention (Pielou 1991; Webb & Bartlein 1992; Gates 1993; Clark *et al.* 1998; Hewitt 2003; Lomolino *et al.* 2006). A vast body of direct historical evidence from the fossil and pollen records clearly demonstrates that many terrestrial species have undergone large and rapid latitudinal shifts in response to Pleistocene climate change, particularly following the end of the last glacial maximum (LGM) approximately 20 000 years before present (ybp) (e.g. Huntley & Birks 1983; Cwynar & MacDonald 1987; Bennett *et al.* 1991; Gates 1993; Graham *et al.* 1996; Bennett 1997; Williams *et al.* 1998; Hewitt 1999). An abundance of fossil and pollen data from eastern North America and western

Correspondence: Peter B. Marko, Fax: 1 864 656 0435; E-mail: pmarko@clemson.edu

Europe provide an empirical basis for an 'Expansion–Contraction' (EC) model of Pleistocene biogeography (Provan & Bennett 2008) that describes the geographic responses of species to past glacial-interglacial climate changes. Under the basic EC model, most northern hemisphere cool-temperate species survived in southern glacial refugia, only re-populating higher latitudes through range expansions following the LGM (Hewitt 2004). In addition to forming a fundamentally important paradigm of Pleistocene biogeography, the EC model also provides a potentially useful model for understanding how species assemblages will respond to climate change in the future (Gates 1993).

Although Pleistocene EC histories are widely documented on land, few studies have characterized the recent biogeographic histories of marine species with the fossil record. Comparable paleontological studies of marine ecosystems over sufficiently similar intervals are rare because of the limitations of the record. For example, although nearly all fossilizable nearshore marine species on the west coast of North America are captured in the Pleistocene (Valentine 1989; Lindberg & Lipps 1996), the record is primarily composed of deposits created during sea-level high-stands associated with relatively warm interglacials; fossils preserved during glacial low-stands are largely unavailable due to the current end-Holocene sea-level high-stand. Existing fossils from cooler climates, that have been exposed by uplift, yield equivocal results. For example, although Addicott (1966) provided evidence of southward shifts of entire biogeographic provinces along the west coast of North America during the LGM, Valentine & Jablonski (1993) later showed that some eastern Pacific species responded to Pleistocene climate change in a much more individualistic manner, resulting in substantial and unpredictable changes in community composition.

In addition to range changes that can be directly documented in the fossil record, the EC model also gives rise to predictions routinely tested with genetic data: populations in recently colonized northern regions should retain the genetic signature of distinctly short demographic histories, consistent with massive population expansions following the end of the LGM (reviewed by Hewitt 2001, 2004; Hewitt & Ibrahim 2001; Emerson & Hewitt 2005). Not surprisingly, interpretations of mitochondrial DNA (mtDNA) studies on land largely meet the expectations of the EC model for many northern hemisphere taxa (e.g. Ibrahim *et al.* 1996; Comes & Kadereit 1998; Taberlet *et al.* 1998; Hewitt 1999), essentially echoing patterns in the fossil and pollen records, with some exceptions. Compared to terrestrial plants and animals, however, available genetic data from marine assemblages tend to suggest that the response to past climate change, particularly to the LGM, has been less uniform across taxa with some species showing patterns of differentiation and divergence consistent with long-term regional persistence (e.g. Hickerson & Ross 2001; Wares & Cunningham 2001; Marko 2004; Hickerson & Cunningham 2005; Hoarau *et al.* 2007). Although a smaller sampling of marine species may bias this pattern, the apparent variability in marine biogeographic histories could also reflect a fundamental difference in the way climate change is experienced by coastal marine species, particularly those living in intertidal habitats. Because of the high degree of small-scale spatial heterogeneity in thermal environments experienced by rocky-shore species, simple climate-driven, latitudinally-related shifts in abundance and geographic range may not always occur, so that the overall demographic and geographic responses of rocky-shore assemblages to climate change may in fact be different from those on land (Helmuth *et al.* 2002).

To address the question of marine organisms' responses to late-Pleistocene climate change, we conducted a community-level comparative genetic analysis of multiple co-distributed rocky-shore species along the Pacific coast of North America. By combining new sequences with previously published data, we have assembled a database of mitochondrial and nuclear DNA sequences from 14 species spanning four animal phyla. Rocky-shore communities present an ideal model with which to investigate the historical ecology of species assemblages given that these ecosystems have provided many rich insights into the responses of organisms to their local biotic and abiotic environments, engendering many important conceptual advances in the field of community ecology (see reviews by Paine 1977, 1994; Paine & Levin 1981; Raffaelli & Hawkins 1999; Menge & Branch 2001). Despite a deep understanding of the biotic and abiotic factors influencing the local abundance and distribution of species on rocky shores, comparatively little is known about the regional persistence of these model assemblages over time scales greater than approximately 30 years and spatial scales larger than a few meters (Valentine & Jablonski 1993; Paine & Trimble 2004). If the EC model best characterizes most species' biogeographic responses to past climate change, then we expect the majority of species should show a strong population genetic signature of population expansion in the temporal vicinity of the LGM, as has been often documented on land (see reviews by Hewitt 1999, 2000, 2004). Our analyses of DNA sequence data from 14 co-distributed rocky-shore species deviate from this expectation, providing a novel perspective on the relationship between climate change and demography in a model marine community.

Methods

By gathering new sequences and retrieving previously published data from GenBank, we assembled a DNA sequence database for 14 co-distributed rocky-shore species in the northeastern Pacific (Table 1). The sampling of taxa spans four animal phyla: Echinodermata (three sea stars), Mollusca (four snails and two bivalves, one chiton), Arthropoda (two barnacles), and Chordata (two fish). The samples are from 25 localities between Kodiak Island, Alaska and Cape Flattery, Washington (Fig. 1, Table S1). Our study focused on the northern two-thirds of the species' ranges (Cape Flattery, Washington to Kodiak Island, Alaska) because few of the taxa we considered have been sampled outside this region (Fig. 1) plus we expected that northern populations should show the strongest evidence of glacial-interglacial demographic change.

We collected new mtDNA sequences from ten species, creating six entirely novel data sets and supplementing four previously existing data sets that typically had only 1–2 samples from British Columbia and Alaska (Tables 1 and S1). For nine of the 14 species, mtDNA data consisted of cytochrome *c* oxidase-1 (CO1) sequences, amplified with universal primers (Folmer *et al.* 1994). Cytochrome b (CytB) was sequenced from *Littorina sitkana* and *L. scutulata*, a portion of the mtDNA control region was sequenced for both species of *Xiphister*, and the mtDNA for *P. miniata* consisted of several mitochondrial transfer RNAs (tRNAs) plus a small portion (54 bp) of the 5′ end of CO1. We collected a completely new CytB data set for *L. sitkana* because previously published sequences (Kyle & Boulding 2000) form a divergent monophyletic clade with a pseudogene sequence in GenBank that contains stop codons (Accession No. U46821, Reid *et al.* 1996). We used the same primers as the previous *Littorina* population study ('EGB-F' and 'EGB-R'), but our methods differed in that we extracted DNA from foot tissue rather than visceral mass (Kyle & Boulding 1998, 2000), which we have found to yield little high-quality mtDNA; additionally, molluscan extractions consisting of gonadal tissue may not contain exclusively female mtDNA if inheritance is not strictly maternal. All DNA extraction and mtDNA amplification protocols followed previously published methods, which consisted of overnight proteinase K incubation in 2X CTAB followed by two chloroform extractions and precipitation with ethanol (see Table 1 for references to sequence sources and methods).

We also collected nuclear elongation factor 1-α (EF1) sequences from the acorn barnacle *Balanus glandula* (see Table S1 for localities) using previously published

Table 1 MtDNA sequence data, mutation rates (substitutions per locus per year) and generation times (years) for 14 northeastern Pacific rocky shore taxa

	Base pairs	Sequence sources	Mutation rate, per locus*	Reproductive maturity (years)	Maturation references
Mollusca					
Mytilus trossulus	661	1	6.61×10^{-6}	0.167	8
M. californianus	661	1	6.61×10^{-6}	0.667	8
Nucella ostrina	607	1, 5	6.07×10^{-6}	1	13
N. lamellosa	586	1, 5	5.86×10^{-6}	4	14
Katharina tunicata	659	1	6.59×10^{-6}	2	15
Littorina sitkana	433	1	4.33×10^{-6}	1	16
L. scutulata	480	6	4.80×10^{-6}	1	16, 17
Arthropoda					
Balanus glandula	405	1, 2	4.05×10^{-6}	0.5†	9, 10
Semibalanus cariosus	659	1	6.59×10^{-6}	2†	11
Echinodermata					
Pisaster ochraceus	543	1, 3	5.43×10^{-6}	5	12
Evasterias troschelii	623	1	6.23×10^{-6}	5	12
Patiria miniata	370	4	3.70×10^{-6}	2	—
Chordata					
Xiphister mucosus	621	7	6.21×10^{-6}	1	7
X. atropurpureus	457	7	4.57×10^{-6}	1	7

1, Present study; 2, Wares & Cunningham (2005); 3, Harley *et al.* (2006); 4, McGovern *et al.* (in preparation); 5, Marko (2004); 6, Kyle & Boulding (2000); 7, Hickerson & Cunningham (2005); 8, Suchanek (1981); 9, Connell (1970); 10, Hines (1978); 11, Barnes (1989); 12, Menge (1974); 13, Spight (1982); 14. Spight (1975); 15, Nimitz and Giese (1964); 16, Mastro *et al.* (1982); 17, Hohenlohe (2002).
*Based on a common 1.0×10^{-8} per site per year rate.
†Values are estimates of generation times for *B. glandula* and *S. cariosus*.

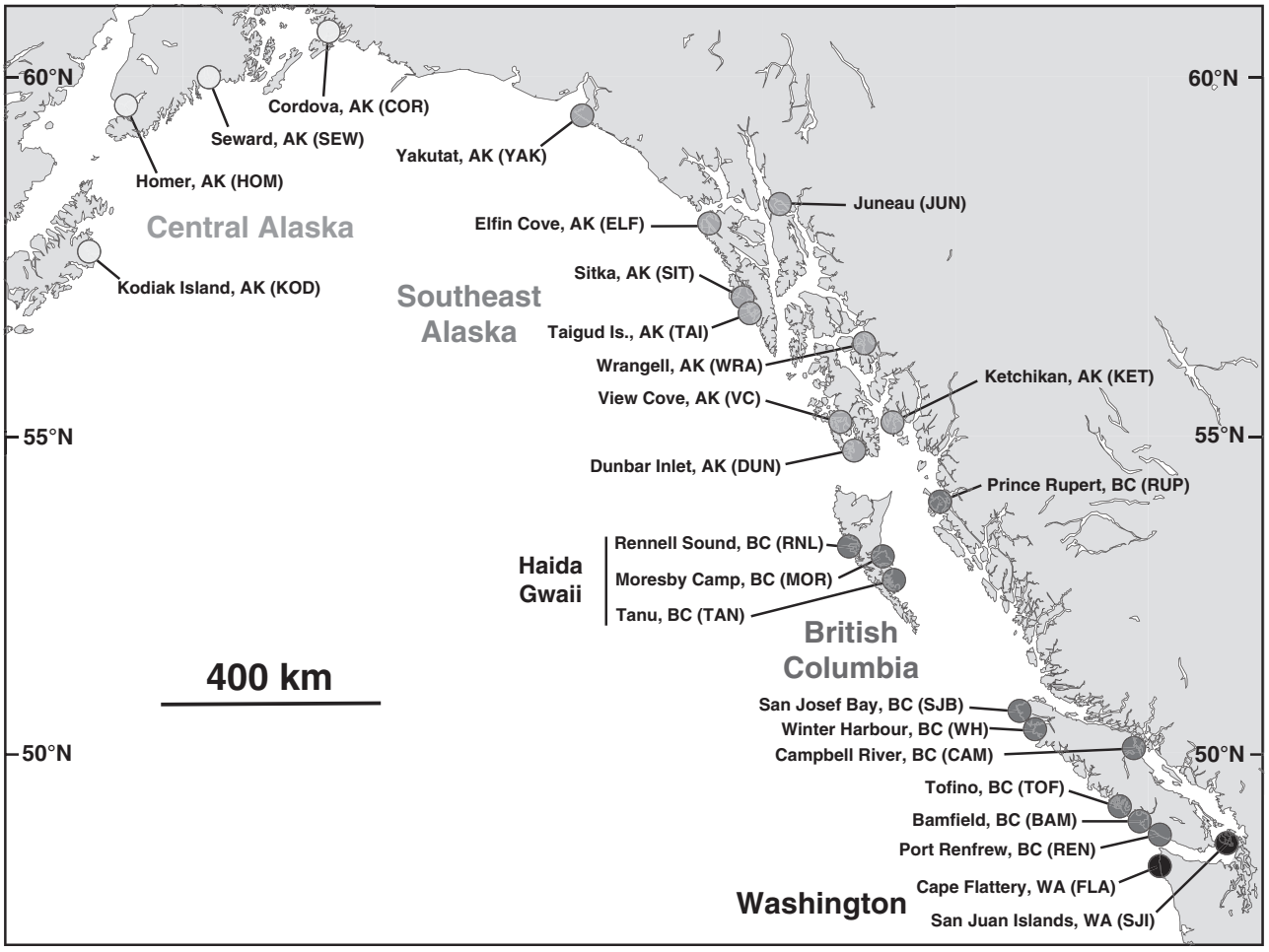

Fig. 1 Collection sites for 14 rocky shore species. Some collection sites have been subsumed into single names due to the size of the diagram. See Table 1 for references to previously published sequences and exact localities; sample sizes of individual localities are provided in Supplementary Table S1.

methods (Sotka *et al.* 2004), re-analyzed sequences electronically retrieved from GenBank from six anonymous nuclear loci from each of the frilled dogwhelk *Nucella lamellosa* and the bat star *P. miniata* (McGovern *et al.*, in preparation), and retrieved and analyzed previously published nuclear α-enolase and α-tropomyosin intron sequences from the two pricklebacks, *X. atropurpureus* and *X. mucosus* (Hickerson & Cunningham 2005). Nuclear DNA data were obtained with a combination of direct sequencing of PCR products and cloning and re-sequencing of putative heterozygotes. For *N. lamellosa* and *B. glandula,* nuclear insertions and deletions ('indels') were uncommon, so heterozygous nucleotide sites were most often scored in chromatograms generated from direct sequencing of PCR products followed by gametic phase determination using the software PHASE 2.1 (Stephens *et al.* 2001) once a sufficient number of heterozygotes were cloned to be confident in this approach; any individuals with putative heterozygous base-calls that did not show a very clear double-peak in both complimentary electropherograms were cloned and re-sequenced. In contrast, owing to greater indel variation, most of the alleles from anonymous loci in *P. miniata* were cloned and re-sequenced.

Because population genetic analyses typically assume no intra-locus recombination, we first tested the nuclear loci for evidence of recombination using IMgc (Woerner *et al.* 2007), a program that uses violations of the 'four-gamete test' (Hudson & Kaplan 1985) to identify the largest data-rich recombination-filtered block of sequences for each locus. We then used the largest contiguous, and presumably unrecombined, block from each species for all further analyses. Each mitochondrial and nuclear data set was next analyzed with ModelTest version 3.7 (Posada & Crandall 1998) and PAUP* version 4.0 (Swofford 2002) to determine the best-fitting DNA substitution model and substitution parameters. We then used Arlequin version 3.11 (Excoffier *et al.* 2005)

to calculate standard molecular diversity indices, Tajima's D, and Fu's F_s; Ramos-Osins & Rozas' R_2 was also calculated using DnaSP version 4.10 (Rozas *et al.* 2003). The significance of empirical values of D, F_s, and R_2 were tested by comparison of observed values to null distributions generated from either 10 000 permutations (Arlequin) or simulations (DnaSP) of the data. Population genetic structure was characterized by calculating Φ_{ST} with Analysis of Molecular Variance (AMOVA) as implemented in Arlequin using the most appropriate substitution model available and parameter values inferred with ModelTest. Haplotype networks were constructed with PAUP*.

For most species, mtDNA AMOVAs using collection sites as subpopulations showed a high degree of genetic homogeneity across sample localities: in nine of 14 species, Φ_{ST} was not statistically different from zero. Because within population variability was of similar magnitude for these nine species, we treated these species lacking any population subdivision as a single unit for demographic analysis (Lessios *et al.* 2001). For the remaining five species that showed significant spatial subdivision, we used pairwise values of Φ_{ST} among samples to create groups of geographically proximate samples that showed no significant differentiation (Waples & Gaggiotti 2006) so that demographic analyses could be limited to groups of adjacent samples that lacked any internal subdivision. Although gene flow among these groupings can potentially bias estimates of effective population size (N_e) upwards, the impact of gene flow should be minimal because nearly all shared haplotypes among the groupings were central haplotypes (i.e. putatively ancestral) within haplotype networks. Some mtDNA samples (see Supplementary Table S1) were too small (<10) to adequately characterize sequence diversity (Pluzhnikov & Donnelly 1996), so we iteratively compared the impacts of including or excluding small samples plus combining them with samples from adjacent (<10 km) localities. These additional analyses had no qualitative impact on any of the results.

We used two methods to characterize the magnitude and timing of past changes in population size. First, we conducted mtDNA mismatch analyses (Rogers & Harpending 1992) with Arlequin. Each mismatch distribution was compared to a distribution expected under a model of sudden population expansion, and any deviation from the sudden expansion model was evaluated by calculating Harpending's (1994) Raggedness Index (r); the significance of r was assessed with 10 000 parametric bootstraps. For each distribution that did not deviate significantly from the sudden expansion model, we calculated the intrapopulation coalescence time (i.e. time since the start of a population expansion) from the statistic τ with the formula $\tau = 2\mu t$, where t is the number of years since a population expansion and μ is the per locus per year mutation rate. Confidence intervals for estimates of τ were obtained using a parametric bootstrap approach in Arlequin.

Second, because the genealogical structure of a sample of alleles or haplotypes contains information about a population's demographic history (Felsenstein 1992; Kuhner *et al.* 1995, 1998), we also characterized past changes in N_e by generating mtDNA Bayesian Skyline Plots (BSPs) with BEAST version 1.4.8 (Drummond *et al.* 2005; Drummond & Rambaut 2007). BEAST employs a Markov chain Monte Carlo (MCMC) sampling procedure that generates a posterior probability distribution for N_e through time based on the temporal distribution of coalescences in gene genealogies, moving backward from the present. Because the method used in BEAST requires the assumption that alleles or haplotypes are sampled from a single population, we only created BSPs for species that showed no spatial subdivision. For each species, we ultimately completed three replicate MCMC searches, each with 100 million steps, trees and parameters sampled every 500 steps, and with a burn-in of 10 million steps. Results from three replicate runs were then combined and re-sampled with LOGCOMBINER version 1.4.8 (Drummond & Rambaut 2007) prior to analysis with TRACER version 1.4.1 (Drummond & Rambaut 2007). TRACER yields estimates of N_eT over time, where T = generation time. Although age of first reproduction is known for most of the taxa in our study, generation times are generally not (but see Connell 1970 for barnacles). Because we were most interested in the timing of relative changes in N_e for each species, rather than the absolute values of N_e, we reported unadjusted values included N_eT in demographic reconstructions, but include values of reproductive maturity for each species. Confidence intervals for N_eT were calculated from the posterior probability distributions using TRACER. For several species, the genealogical structure of the haplotype networks indicated the possibility that multiple colonization events involving distinct haplotype lineages may have potentially upwardly biased our estimates of ancestral population size, particularly for species with long-lived planktonic larvae and presumably high gene flow from southern refugia. We therefore repeated the demographic analyses for several subclades within species whose haplotype networks contained more than one well-represented distinct lineage.

To assess whether the BSP was the most appropriate model for reconstructing demographic histories, we compared each BSP to demographic reconstructions under two simpler models in BEAST: constant population size and a two-epoch model of expansion growth

(a period of constant size followed by a period of exponential). The comparisons were conducted with Bayes Factor Tests in TRACER by importance sampling of the marginal likelihoods of each of the three models (Newton & Raftery 1994; Suchard *et al.* 2001; Redelings & Suchard 2005). BEAST runs for the two alternative demographic models were conducted in the same way as described above for the BSP. The strength of support from Bayes Factors was interpreted using guidelines from Jeffreys (1961).

The currently available version of BEAST cannot generate demographic reconstructions from multilocus data. Therefore, we also estimated population divergence times among geographically adjacent samples of the five species with multilocus sequence data using the isolation with migration model implemented in IMA (Hey & Nielsen 2004, 2007). IMA is a coalescent-based method that uses MCMC simulations of gene genealogies to estimate the time of divergence (t), genetic diversities (Θ_1, Θ_2, and ancestral Θ_A), and migration rates (m_1 and m_2) between two populations assumed to have shared a common ancestor. For each pair of samples, we first optimized and conducted a run under 'MCMC Mode' using the fully parameterized isolation with migration model (i.e. six parameters: Θ_1, Θ_2, Θ_A, m_1, m_2, t). We next used likelihood ratio tests implemented in the nested model option in 'Load Trees Mode' to compare the likelihood of simpler models (e.g. three parameters: $\Theta_1 = \Theta_2 = \Theta_A$, $m_1 = m_2$, t) to the fully parameterized model. The best fitting model was then used to infer the divergence time between samples. For each individual IMA analysis, we initially used broad prior probabilities for population parameters and then subsequently reduced the upper limits in repeated runs of the program. Convergence was assessed by monitoring the effective sample size, examining parameter trend plots, and, most importantly, conducting three final replicate runs, each starting with a different random seed. Replicate runs were inspected for consistency and then re-sampled using the Load Trees Mode in IMA for final parameter estimation.

To re-scale results into units of years, we first considered mutation rates reported in the literature. Given that the vast majority of mtDNA divergence rate estimates across the phyla we have considered fall within 0.7–2.4%/MY (e.g., Collins *et al.* 1996; Reid *et al.* 1996; Knowlton & Weigt 1998; Wares & Cunningham 2001; Marko 2002; Hickerson & Cunningham 2005; Lessios 2008), we opted to base our mutation rate on the relatively rapid divergence rate of 2% per MY (equivalent to a mutation rate of 1.0×10^{-8} substitutions per site per year) for all of the taxa. Slower rates have been inferred for marine taxa, including some of the taxa and mtDNA regions in our study (Hart *et al.* 1997; Hickerson & Cunningham 2005; Frey & Vermeij 2008), but conversion of population genetic parameters with the relatively fast 2% rate was expected to yield conservative results with respect to our conclusions: slower mutation rates would increase divergence time estimates and make inferred population expansion times older. With multilocus data sets, IMA only requires knowledge of the mutation rate for one (i.e. mtDNA) locus. However, to generate a BSP for EF1 from *B. glandula*, we assumed that the mutation rate of this nuclear locus was an order of magnitude smaller than the mtDNA locus.

Results

Sequence diversity

Summary statistics for mtDNA drift-mutation equilibrium tests (D, R_2, and F_s) in Table 2 showed strong departures from equilibrium expectations in nearly all of the species, meaning that most species showed significant evidence of either past selective sweeps or population expansions. Only *L. sitkana* and *X. mucosus* lacked significant values for any of these statistics, but this result was probably caused by a near absence of any haplotype and nucleotide diversity in these two species (Table 2). Nuclear sequences from five of the species showed fewer significant values for mutation-drift equilibrium statistics (Table 3), but at least one statistic was significant for most loci.

Population structure

Nine of the 14 species in our mtDNA survey showed an absence of significant spatial genetic structure whereas five exhibited values of Φ_{ST} significantly different from zero (Table 2). Although the sea star *P. ochraceus* showed a significant value of Φ_{ST} ($P = 0.0275$) across all samples (Table 2), inspection of pairwise values of Φ_{ST} among samples showed that only Cordova, at the northern end of the species' distribution, was significantly differentiated from the other samples in our analysis. Because exclusion of the Cordova sample caused the global Φ_{ST} to drop to 0.008 ($P = 0.3429$), we conducted demographic analyses on the Cordova sample separately and for all of the remaining localities combined for *P. ochraceus* (we note here that samples of *P. ochraceus* from southern Puget Sound have also been shown to be differentiated from the San Juan Islands and from outer coast samples [Harley *et al.* 2006]; however, those samples were not included in our analysis because the sampling of the other 13 species did not extend as far south into Puget Sound).

Table 2 MtDNA Sample size (n), nucleotide diversity (π), haplotype diversity (h), Tajima's D, Fu's F_s statistic, Ramos-Osins and Rozas' R_2 statistic, Φ_{ST} from AMOVA analysis, Harpending's Raggedness statistic (r), and values of τ estimated from a sudden expansion model (with 90% credibility intervals in parentheses). Boldface indicates statistically significant values. For species with significant spatial structure (i.e. Φ_{ST}), values of r and τ were calculated for individual sample localities (see Fig. 6). See Supporting Information for sample localities and sizes

Species	n	π	h	D	F_s	R_2	Φ_{ST}	r	τ
Evasterias troschelii	79	0.0007	0.335	**−2.31**	**−12.7**	**0.037**	−0.007	0.167	0.39 (0.13–1.11)
Mytilus californianus	75	0.0062	0.981	**−2.61**	**−63.5**	**0.021**	0.004	0.018	4.14 (2.76–4.73)
M. trossulus	141	0.0057	0.953	**−2.34**	**−96.4**	**0.021**	0.009	0.017	2.36 (1.30–4.52)
Balanus glandula	140	0.0099	0.938	**−2.01**	**−90.1**	**0.032**	0.0003	0.010	2.70 (1.39–5.44)
Semibalanus cariosus	125	0.0033	0.868	**−2.24**	**−54.4**	**0.022**	0.025	0.041	1.49 (1.08–2.99)
Katharina tunicata	74	0.0085	0.833	−0.25	**−5.18**	0.095	−0.037	0.039	5.96 (3.55–11.6)
Littorina sitkana	96	0.0003	0.141	−0.87	−0.03	0.029	0.006	0.539	0.14 (0.00–0.87)
L. scutulata	248	0.0021	0.327	**−2.19**	**−11.6**	**0.018**	0.004	0.356	1.78 (0.00–4.14)
Xiphister mucosus	24	0.0005	0.228	0.25	0.67	0.068	0.086	0.347	0.26 (0.08–1.39)
X. atropurpureus	46	0.0279	0.961	0.14	**−11.0**	0.091	**0.296**	—	—
Pisaster ochraceus	179	0.00104	0.188	**2.28**	**23.9**	**0.015**	**0.104**	—	—
Nucella ostrina	102	0.00155	0.521	**−1.83**	**8.85**	**0.029**	**0.259**	—	—
N. lamellosa	137	0.00328	0.775	**−2.56**	**−25.5**	**0.022**	**0.066**	—	—
Patiria miniata	181	0.0027	0.706	**−1.77**	**−13.7**	0.031	**0.265**	—	—

Table 3 Nuclear DNA sample sizes (n), nucleotide diversity (π), haplotype diversity (h), Tajima's D, Fu's F_s statistic, Ramos-Osins and Rozas' R_2 statistic, and Φ_{ST} from AMOVA analysis estimated from a sudden expansion model (with 90% credibility intervals in parentheses). Boldface indicates statistically significant values. See sequence sources and Supporting Information for sample localities

	Base pairs*	Sequence source†	n	π	h	D	F_s	R_2	Φ_{ST}
Balanus glandula									
EF1-α	312	1	167	0.0038	0.503	**−2.17**	**−23.7**	**0.021**	**0.260**
Nucella lamellosa									
A6	448	2	79	0.0018	0.465	**−1.78**	−2.40	**0.035**	**0.403**
A8	254	2	47	0.0069	0.785	−0.89	−1.00	0.079	**0.383**
NL4	616	2	50	0.0013	0.600	**−2.00**	**−7.00**	**0.051**	**0.143**
NL13	257	2	59	0.0017	0.431	**−2.13**	−0.40	0.105	**0.216**
NL16	593	2	69	0.0011	0.565	0.04	−0.04	0.106	−0.021
NL23	487	2	67	0.0121	0.755	1.74	5.15	0.164	**0.422**
Patiria miniata									
A1	398	2	45	0.0341	0.934	**0.37**	**−24.4**	0.085	0.035
A3	504	2	41	0.0034	0.568	**−2.58**	**−26.8**	0.127	**0.229**
A4	296	2	50	0.0142	0.944	**−2.26**	**−25.8**	**0.048**	0.059
A7	485	2	47	0.0823	0.986	0.43	**−20.2**	0.120	0.070
B1	374	2	40	0.0590	0.977	**−1.39**	**−23.4**	**0.048**	0.035
C1	557	2	57	0.0263	0.983	0.08	**−24.3**	0.089	0.032
X. mucosus									
α-enolase	474	3	58	0.0005	0.163	−1.06	−1.65	0.073	0.000
α-tropomyosin	527	3	54	0.0001	0.037	**−1.09**	−1.70	0.135	0.231
X. atropurpureus									
α-enolase	312	3	72	0.0053	0.819	−0.41	−1.67	0.092	**0.114**
α-tropomyosin	352	3	56	0.0034	0.794	−0.85	**−3.12**	0.073	**0.132**

*Number of base pairs in largest non-recombining block of sequences (see Methods).
†Also see Supporting Information, Table S1.
1, Present study; 2, McGovern *et al.* (in preparation); 3, Hickerson & Cunningham (2005).

Three of the five species with nuclear sequence data showed significant values of Φ_{ST} at most loci, and the results were largely consistent with corresponding mtDNA results. For example, the prickleback *X. mucosus* showed no significant spatial differentiation at any locus. For *P. miniata*, however, only one nuclear locus

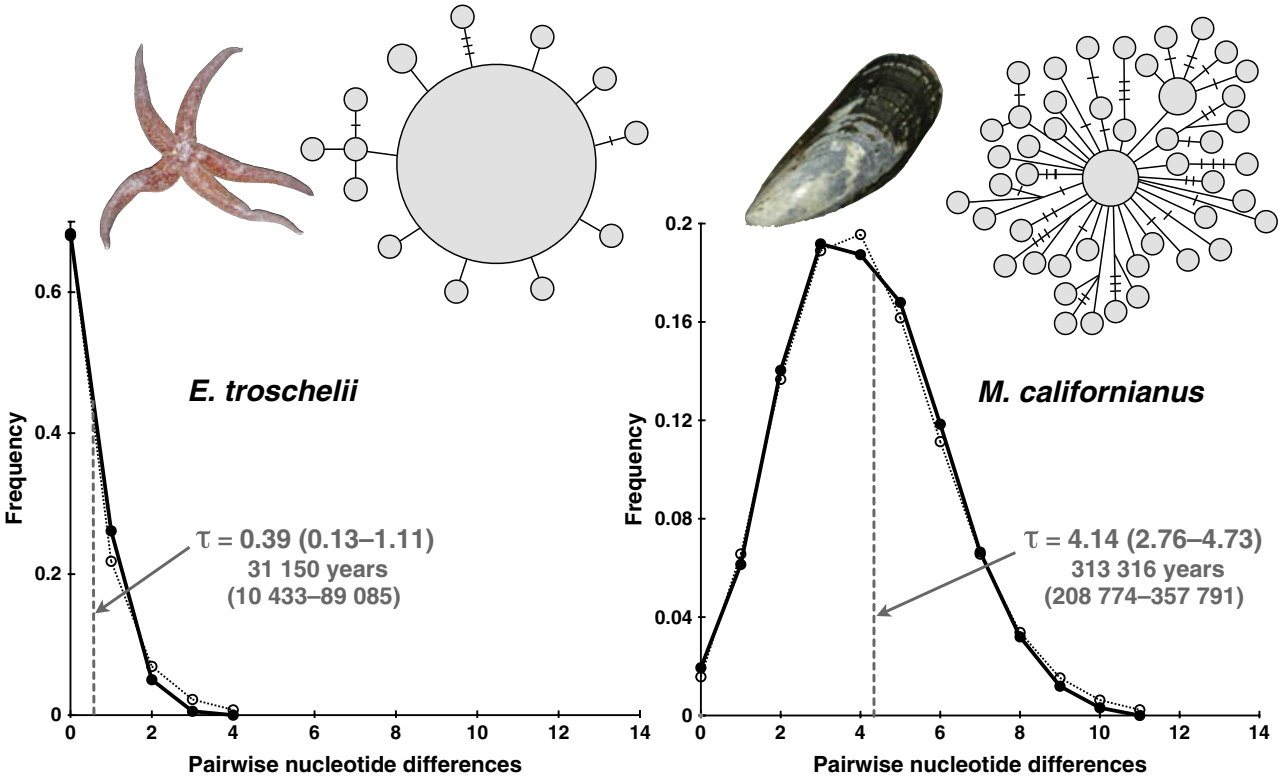

Fig. 2 Exemplar maximum-parsimony mitochondrial DNA haplotype networks, corresponding mismatch distributions (observed values: closed circles, solid lines; expected values: open circles, dashed lines), and approximate intrapopulation coalescence time (τ) for the sea star *Evasterias troschelii* and the mussel *Mytilus californianus*. Confidence intervals for τ were estimated with a parametric bootstrap approach in Arlequin. Each branch in the networks represents one inferred mutational step; slashes across branches indicate additional mutations. The smallest circles within each network correspond to a single haplotype copy.

showed significant differentiation in comparison to a large and highly significant value of Φ_{ST} from the mtDNA. Although smaller values of Φ_{ST} from nuclear data were expected given the four-fold difference in N_e between nuclear and mitochondrial markers, the sampling of each nuclear locus in *P. miniata* (<10 sequences at some locations) may also not have been sufficiently large to detect spatial subdivision in a species with long-lived planktonic larvae (Pluzhnikov & Donnelly 1996). The barnacle *B. glandula* showed the greatest discrepancy between patterns of spatial mtDNA and nuclear subdivision given that the mtDNA data showed no spatial structure (Φ_{ST} = 0.0003) but nuclear EF1 showed a large and statistically significant value of Φ_{ST} (Φ_{ST} = 0.260). Subdivision at EF1 was uniform across the region, with many significant pairwise values of Φ_{ST} but no obvious clines or breaks as reported in California (Sotka *et al.* 2004).

MtDNA haplotype networks and mismatch analyses

Among species that showed no significant mtDNA population structure, two contrasting mtDNA haplotype networks are shown in Fig. 2 along with their corresponding mismatch distributions for the sea star *Evasterias troschelii* and the California mussel *Mytilus californianus*. Both consist of one relatively common haplotype at the centre of the network with either a few (*E. troschelii*) or many (*M. californianus*) rare haplotypes that differ from the central haplotype by one to five base pair differences. Fig. 2 thus illustrates the relationship between the network structure and the shape of the corresponding mismatch distributions. For example, because most individuals of *E. troschelli* possess the haplotype at the centre of the network, the modal number of differences among haplotypes is zero. In contrast, the network for *M. californianus* has many more haplotypes, including several that differ from the most common haplotype by >4 bp changes. Therefore, the mismatch distribution is shifted to the right for *M. californianus*, consistent with a relatively older demographic expansion.

Both *E. troschelli* and *M. californianus* had smooth and unimodal mismatch distributions (Fig. 2), a pattern consistent with a single demographic expansion in the past. Based on values of Harpending's *r*, neither distribution

represented a significant departure from a model of sudden demographic expansion (Table 2). However, the confidence intervals for estimates of the intrapopulation coalescence time (τ) did not overlap (Fig. 2), indicating that demographic expansions in the two species happened at significantly different times. Conversion of τ into years reveals that although the inferred time for the start of a population expansion in *E. troschelii* of 31 150 years (or 31.2 kyr) was not significantly greater than the LGM 20 kyr ago, the sudden expansion start time in *M. californianus* (313 kyr) was significantly older than the LGM. Some of the other species' mtDNA haplotype networks were variants on the two networks in Fig. 2, but others were more complex, consisting of two or three common haplotypes with an abundance of closely related but rarer haplotypes (Fig. 3). Nevertheless, the sudden expansion model could not be rejected for any of the other 12 species (Table 2).

The shapes of mismatch distributions varied considerably among the other 12 species (Fig. 4), indicating a diversity of histories, albeit each consistent with a demographic expansion at some time in the past. In addition to *E. troschelii*, four other species' mismatch distributions (*L. sitkana*, *X. mucosus*, *P. ochraceus*, & *L. scutulata*) showed a large peak at the origin (Fig. 4), reflecting that for each of these species, most individuals possessed the same haplotype across the roughly 2000 km stretch of coastline that we sampled. Two of these species with modal mismatch values of zero (*P. ochraceus* & *L. scutulata*) also showed small secondary peaks created by the presence of a small number of relatively divergent haplotype lineages. For *P. ochraceus*, the secondary peak was generated by the presence of a single divergent lineage found only at Sitka and Cordova, whereas the secondary peak for *L. scutulata* was caused by the presence of a divergent clade with haplotypes present at several sites near Bamfield, Cape Flattery, and Sitka. The mismatch distribution for the genetically differentiated Cordova sample of *P. ochraceus* (not shown) was similar to that for all of the other samples combined, and although differentiated from all samples to the south, the Cordova sample also showed a similar intrapopulation coalescence time ($\tau = 0.459$, CI: 0–0.660, $r = 0.369$, $P = 0.957$) to the other samples from this species ($\tau = 0.592$, CI: 0.455–0.814, $r = 0.131$, $P = 0.245$). In addition to *M. californianus,* four species (*S. cariosus, M. trossulus, B. glandula*, and *K. tunicata*) showed non-zero peaks in their mismatch distributions (Fig. 4).

After re-scaling τ with the mutation rates in Table 1, the time since the start of a population

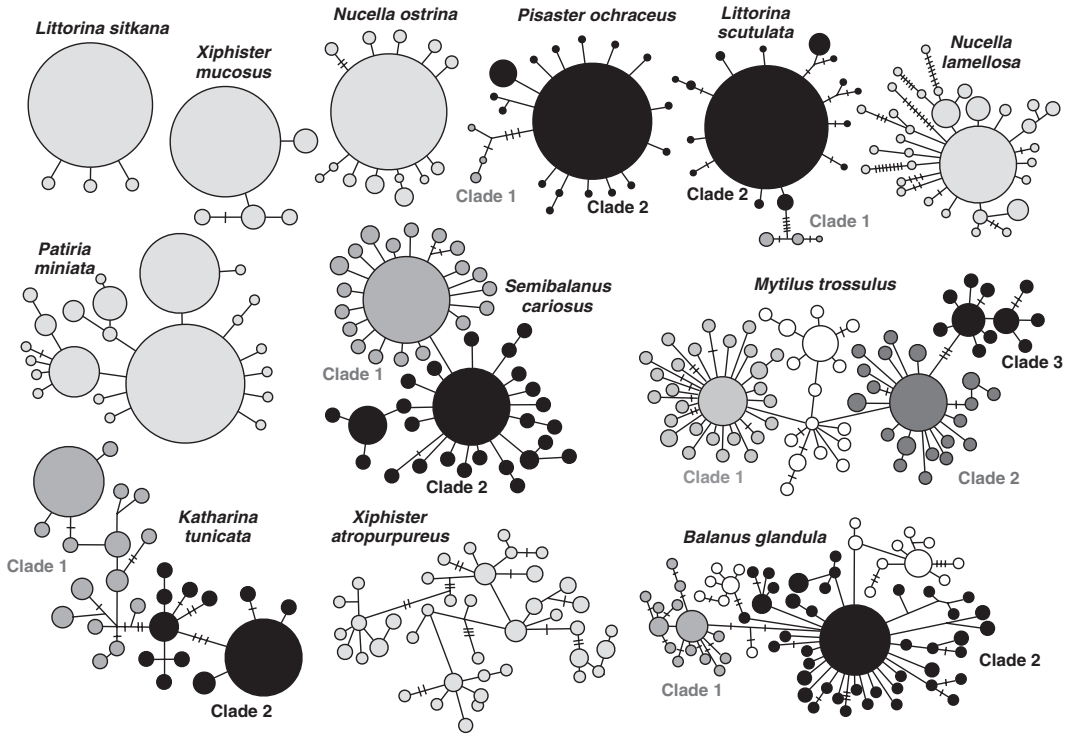

Fig. 3 Maximum-parsimony mitochondrial DNA haplotype networks for twelve rocky-shore northeastern Pacific species. Each branch in the networks represents one inferred mutational step; slashes indicate additional mutations. The smallest circles within each haplotype network correspond to a single haplotype copy.

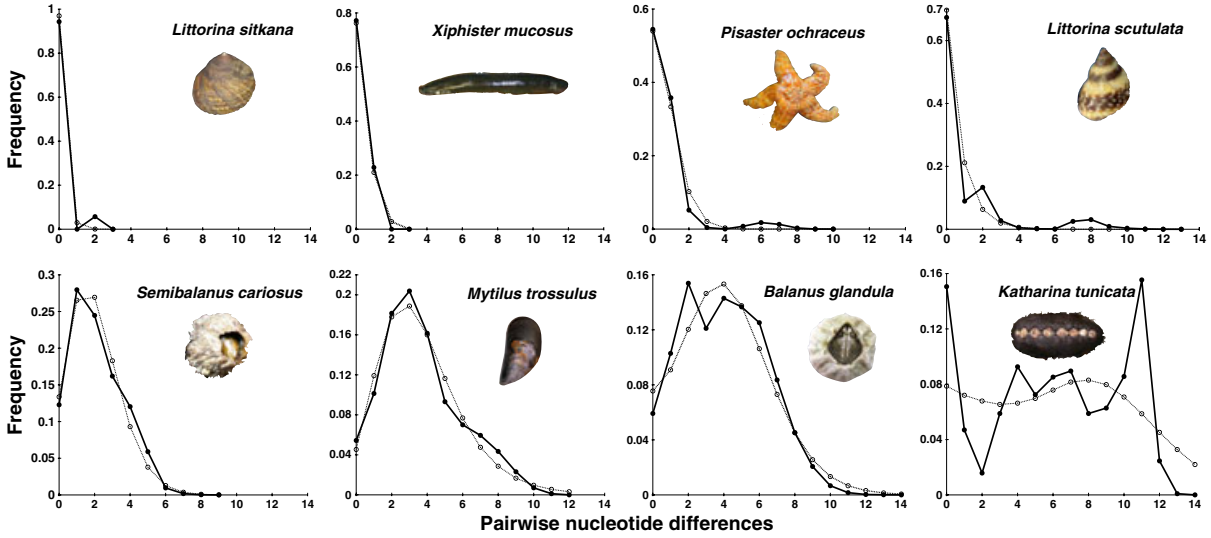

Fig. 4 Observed (closed circles, solid lines) and expected (open circles, dashed lines) mitochondrial DNA mismatch distributions for species lacking spatial mitochondrial DNA genetic structure.

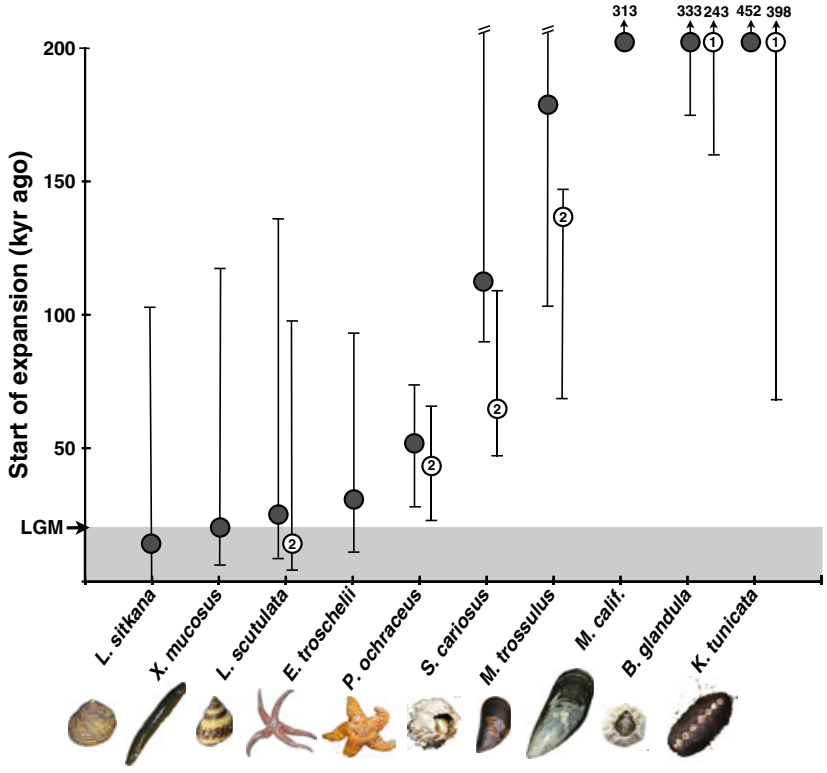

Fig. 5 Population expansion start times (in thousands of years or kyr) and corresponding confidence intervals inferred from mitochondrial DNA for species lacking spatial mitochondrial DNA structure. Confidence intervals calculated with a parametric bootstrap approach in Arlequin. Closed circles represent expansion start times inferred from the complete haplotype data set for each species. Open circles represent the youngest expansion start time inferred from any individual clade; numbers inside the circles correspond to clades in Fig. 3. The grey rectangle at the bottom of the diagram represents the period of time since the last glacial maximum (LGM).

expansion in each spatially unstructured species varied from a low of 16.2 kyr in *L. sitkana* to a high of 452 kyr in *K. tunicata* (Fig. 5). Expansion times for five species (*L. sitkana*, *X. mucosus*, *L. scutulata*, *E. troschelii*, & *P. ochraceus*) are relatively close to the end of the LGM, with confidence intervals for four overlapping with the LGM (Fig. 5). However, for the other five species (*S. cariosus*, *M. trossulus*, *M. californianus*, *B. glandula*, & *K. tunicata*), population expansion times substantially pre-dated the LGM; the lower bounds on the confidence intervals for these estimates were all older than the LGM (Fig. 5). For species that possessed more than one distinct haplotype lineage, expansion times for individual clades were younger, but not inconsistent with the dates inferred from the complete haplotype data sets (Fig. 5). Among the four species which showed significant spatial genetic structure (*N. ostrina*, *N. lamellosa*, *P. miniata*, and *X. atropurpureus*), regional mismatch analyses for groups of adjacent samples that showed no genetic differentiation yielded a diversity of population expansion start times, the majority of which pre-dated the LGM (Fig. 6). For two of these species (*N. lamellosa* & *N. ostrina*), the population expansion times for the northernmost samples were both consistent with a large post-LGM demographic expansion.

Bayesian demographic reconstructions

Among species that showed no spatial mtDNA genetic structure, mtDNA Bayesian Skyline Plots (BSPs) were generally consistent with the results from the mismatch analyses. Among the five species whose expansion times from mismatch analyses were broadly consistent with LGM recolonization (Fig. 5), BSPs for *E. troschelii* and *P. ochraceus* showed very large (>10 fold) increases in N_e over the last 20 kyr (Fig. 7). However, the BSP for *L. scutulata* (Fig. 7) showed a much less dramatic increase in N_e towards the present than either *P. ochraceus* or *E. troschelii* despite a modal mismatch value of zero for *L. scutulata* (Fig. 4). A BSP for *L. scutulata* based only on Clade 2 (see Fig. 3) also lacked any clear signature of recent growth, but did show a relatively short coalescent history (Fig. 8). For two other species with very low mtDNA diversities (*L. sitkana* & *X. mucosus*), BSPs were also similarly uninformative (not shown in

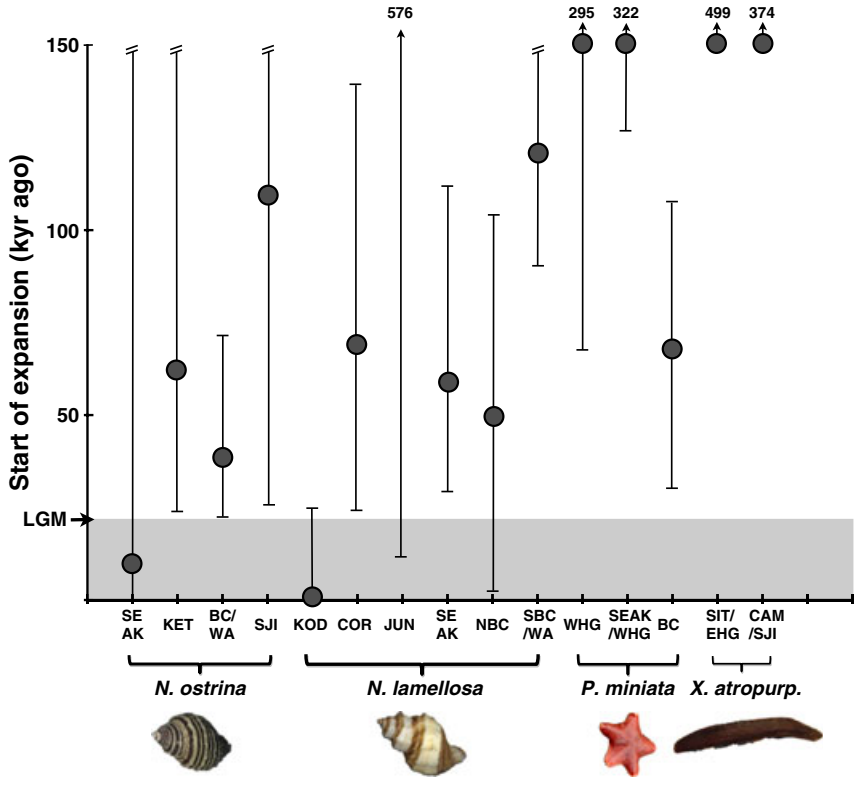

Fig. 6 Regional population expansion start times (in thousands of years or kyr) and corresponding confidence intervals inferred from mitochondrial DNA for species that exhibited significant spatial mitochondrial DNA. Abbreviations are as in Fig. 1 except: SE AK, southeast Alaska; BC, British Columbia; NBC, Northern BC (north of Vancouver Island); WA, Washington; WHG, western Haida Gwai; EHG, eastern Haida Gwai. The grey rectangle corresponds to the period of time since the last glacial maximum (LGM).

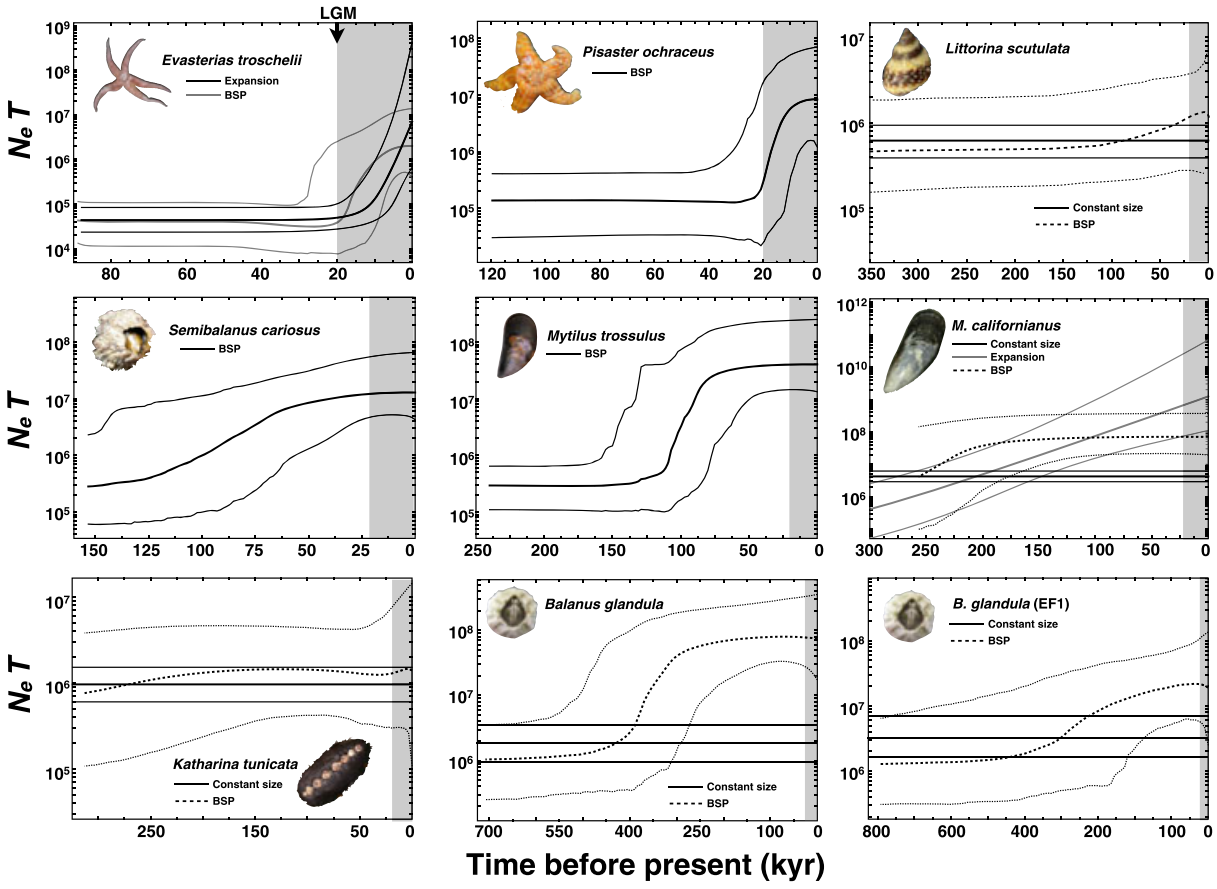

Fig. 7 Bayesian demographic reconstructions (N_eT, where N_e = effective population size and T = generation time) over time (in thousands of years or kyr) inferred with BEAST for species lacking spatial mtDNA genetic structure. All reconstructions are based on mitochondrial DNA except for elongation factor 1-α (EF1) from *Balanus glandula*. Solid lines (black and grey) represent reconstructions using demographic models favoured by Bayes Factor tests (see Table 4); dashed lines correspond to Bayesian Skyline Plots (BSP) not supported by Bayes factor tests. The scales of both axes vary among plots. The grey rectangle corresponds to the period of time since the last glacial maximum (LGM).

Fig. 6); presumably, these three low diversity data sets have too few mutations to estimate rates of gene coalescence and thus provide little information about rates of change in N_e.

In contrast, BSPs for five species (*S. cariosus*, *M. trossulus*, *M. californianus*, *B. glandula*, & *K. tunicata*) were not consistent with post-LGM expansions, instead showing evidence of either older episodes of population growth or demographic stability (Fig. 7). Although EF1 in *B. glandula* showed a large and significant value of Φ_{ST}, we plotted the demographic reconstruction for EF1 because, like the mtDNA BSP for this species, the EF1 BSP showed evidence of a relatively ancient increase in N_e (Fig. 7). Although the mutation rate we used for EF1 lacks an empirical basis, the EF1 BSP showed no evidence of a recent demographic expansion, even if we assumed that the mutation rate was the same as for the mtDNA (i.e. an order of magnitude larger). BSPs for individual clades within species that possessed more than one distinct haplotype lineage were generally consistent with those based on complete data sets, in that none showed patterns of growth clearly consistent with LGM expansion (Fig. 8).

Bayes Factor (BF) tests (Table 4) for three species (*M. trossulus*, *S. cariosus*, & *P. ochraceus*) showed that the BSP fit the mtDNA data better than the other simpler demographic models considered. For one species' mtDNA (*E. troschelii*), the BSP and expansion models were both a better fit to the data than the constant size model. Although neither the expansion model nor the BSP was a substantially better fit over the other for *E. troschelii* (Table 4), both reconstructions were consistent with LGM-expansion (Fig. 7). Not surprisingly, the constant size model was favoured for three species that showed relatively flat

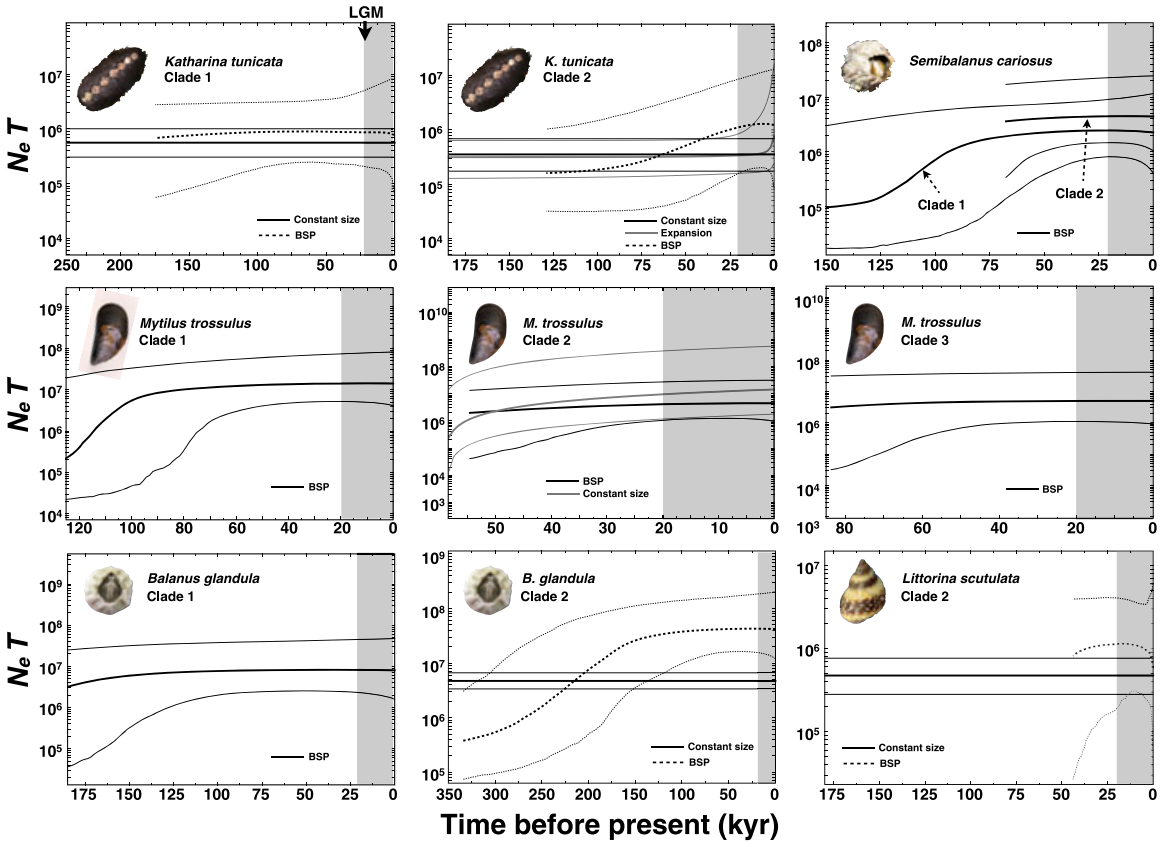

Fig. 8 Bayesian demographic reconstructions (N_eT, where N_e = effective population size and T = generation time) over time inferred with BEAST for species lacking spatial mtDNA genetic structure. All reconstructions are based on individual mitochondrial DNA subclades in Fig. 3. Solid lines (black and grey) represent reconstructions using demographic models favoured in Bayes Factor tests (see Table 4); dashed lines correspond to Bayesian Skyline Plots (BSP) not supported by Bayes factor tests. The scales of both axes vary among plots. The grey rectangle corresponds to the period of time since the last glacial maximum (LGM).

BSPs (*K. tunicata*, *B. glandula*, & *L. scutulata*). The expansion model alone was strongly favoured for one species with extremely low nucleotide diversity (*L. sitkana*), but both the constant size model and the expansion model were each a significantly better fit than the BSP for both *X. mucosus* and *M. californianus* (Table 4). For nuclear EF1 sequences from *B. glandula*, BF tests indicated that, as with the mtDNA from this species, constant size was the best-fitting demographic model given the data.

Overall, in cases where the best-fitting demographic model was a simpler alternative to the BSP, the reconstruction based on the simpler model generally exhibited a similar shape to the BSP (Fig. 7). Not surprisingly, for *M. californianus*, the BSP was an intermediate reconstruction relative to the expansion and constant size reconstructions. Also, even though BSPs for both COI and EF1 from *B. glandula* showed evidence of a large pre-LGM demographic expansion, the constant size model received the most support from BF tests for both loci.

Multilocus population divergence times

The majority of multilocus population divergence times for three (*P. miniata*, *B. glandula*, & *X. atropurpureus*) of five species significantly predated the LGM (Table 5). The only two adjacent samples among these three species that showed a divergence time less than 20 kyr are the View Cove and Dunbar Inlet samples of *P. miniata*, which are separated by less than 100 km in southeast Alaska (Fig. 1). In *N. lamellosa*, although most of the MLEs for population divergence times substantially predated the LGM, the lower bound on the confidence interval overlapped broadly with the LGM in nine out of ten comparisons. In *X. mucosus*, the lone pair of samples from this region showed a relatively recent post-glacial split, consistent with previously published analyses. Even when using a slower mtDNA rate for this species from a biogeographic calibration (Hickerson & Cunningham 2005), the divergence time broadly overlapped with the LGM (not shown).

Table 4 Bayes Factor tests comparing demographic models for 10 northeastern Pacific rocky shore species lacking spatial mtDNA structure. Bayes Factors correspond to row by column comparisons. All comparisons are based on mtDNA data except for *B. glandula* nuclear elongation factor 1 alpha (EF1) sequences. Boldface corresponds to the best fitting demographic model(s)

Species	Model	Ln P(model)	SE	Bayes Factors†		
				BSP	Constant size	Expansion
Evasterias troschelii	**BSP**	−2781.8	0.061	—	3.43*	0.524
	Constant	−2783.1	0.052	0.292	—	0.153
	Expansion	−2781.2	0.055	1.909	6.54*	—
Mytilus trossulus	**BSP**	−1760.3	0.092	—	12.8**	15.5**
	Constant	−1762.9	0.128	0.078	—	1.21
	Expansion	−1763.1	0.14	0.064	0.828	—
M. trossulus Clade 1	**BSP**	−1332.6	0.1	—	3.25*	1.0×10^{113}***
	Constant	−1333.7	0.086	0.308	—	3.1×10^{112}***
	Expansion	−1592.8	0.12	0	0	—
M. trossulus Clade 2	**BSP**	−1084.9	0.063	—	76.2**	1.92
	Constant	−1089.2	0.059	0.013	—	0.025
	Expansion	−1085.5	0.054	0.521	39.7**	—
M. trossulus Clade 3	**BSP**	−1041.6	0.046	—	11.0**	4.89*
	Constant	−1044.0	0.044	0.091	—	0.444
	Expansion	−1043.2	0.048	0.204	2.25	—
M. californianus	BSP	−1634.3	0.124	—	0.018	0.013
	Constant	−1630.3	0.117	55.261**	—	0.695
	Expansion	−1630.0	0.108	79.513**	1.44	—
Balanus glandula	BSP	−1446.9	0.133	—	0	1.52
	Constant	−1426.7	0.169	5.8×10^{9}***	—	8.9×10^{9}***
	Expansion	−1447.3	0.194	0.656	0	—
B. glandula Clade 1	**BSP**	−1162.2	0.054	—	5.319*	4.271*
	Constant	−1163.9	0.062	0.188	—	0.803
	Expansion	−1163.6	0.052	0.234	1.245	—
B. glandula Clade 2	BSP	−1809.1	0.147	—	0	0.047
	Constant	−1799.1	0.131	2.2×10^{4}***	—	1.0×10^{3}***
	Expansion	−1806.0	0.143	21.402	0.001	—
B. glandula EF1	BSP	−722.1	0.196	—	0	0.013
	Constant	−713.2	0.071	7.47×10^{3}***	—	93.6**
	Expansion	−717.7	0.086	79.806	0.011	—
Semibalanus cariosus	**BSP**	−1364.3	0.08	—	15.4**	176.7***
	Constant	−1367.0	0.113	0.065	—	11.5
	Expansion	−1369.4	0.093	0.006	0.087	—
S. cariosus Clade 1	**BSP**	−1067.7	0.075	—	4.78*	3.91
	Constant	−1068.9	0.069	0.288	—	0.838
	Expansion	−1068.7	0.071	0.343	1.194	—
S. cariosus Clade 2	**BSP**	−1096.2	0.083	—	3.446*	4.286*
	Constant	−1097.9	0.067	0.489	—	1.607
	Expansion	−1098.4	0.077	0.304	0.622	—
Katharina tunicata	BSP	−1202.1	0.077	—	0.221	0.817
	Constant	−1200.6	0.072	4.52*	—	3.69*
	Expansion	−1201.9	0.081	1.224	0.271	—
K. tunicata Clade 1	BSP	−1057.2	0.057	—	0.34	0.509
	Constant	−1054.1	0.047	4.94*	—	3.50*
	Expansion	−1056.5	0.051	1.964	0.667	—
K. tunicata Clade 2	BSP	−1013.7	0.054	—	0.048	0.088
	Constant	−1010.7	0.046	20.7**	—	1.82
	Expansion	−1011.3	0.054	4.0×10^{47}***	0	—
Littorina sitkana	BSP	−915.4	0.056	—	0.077	0
	Constant	−912.8	0.053	13.0**	—	
	Expansion	−616.5	0.025	6.1×10^{129}***	4.7×10^{128}***	—

Table 4 *Continued*

Species	Model	Ln P(model)	SE	Bayes Factors†		
				BSP	Constant size	Expansion
L. scutulata	BSP	−958.2	0.118	—	0.046	1.40
	Constant	−955.2	0.098	21.6**	—	30.2**
	Expansion	−958.6	0.112	0.713	0.033	—
L. scutulata Clade 2	BSP	−885.8	0.175	—	0	0.001
	Constant	−876.6	0.09	1.0×10^4***	—	11.6**
	Expansion	−879.0	0.096	865.4***	0.086	—
Xiphister mucosus	BSP	−577.4	0.036	—	−23.19	−22.94
	Constant	−524.0	0.029	23.2**	—	0.254
	Expansion	−524.6	0.030	22.9**	−0.254	—
P. ochraceus‡	**BSP**	−969.8	0.065	—	6.54*	3.74*
	Constant	−971.7	0.07	0.153	—	0.571
	Expansion	−971.1	0.073	0.267	1.75	—

†Strength of Bayes Factor evidence based on Jeffreys (1961): * = substantial; ** = strong; *** = decisive.
‡Cordova sample excluded.

Table 5 Best-fitting models and resulting multilocus estimates of theta (θ), migration (*m*), and population divergence times (*T*, in thousands of years or kyr, with 90% highest posterior density or HPD intervals in parentheses) inferred with the program IMA for adjacent populations of northeast Pacific marine species. Boldface values of T indicate lower 90% HPD exceeded the end of the last glacial maximum (20 kyr).'?' indicates that the upper bound on the posterior probability distribution did not drop to zero; in these cases, the lower bound was taken as the point at which the left side of the distribution dropped to zero

	Best-fitting model	Θ_1	Θ_2	Θ_A	m_1	m_2	*T* (kyr)
Nucella lamellosa							
KOD vs. COR	$\Theta_1, \Theta_2, \Theta_A, m_1 = m_2 = 0$	0.961	0.192	0.965	0	0	45.3 (6.2–173)
COR vs. SIT	$\Theta_1, \Theta_2, \Theta_A, m_1 = m_2 = 0$	0.330	94.4	1.94	0	0	72.8 (17.6–194)
SIT vs. JUN	$\Theta_1, \Theta_2, \Theta_A, m_1 = m_2 = 0$	7.20	0.78	1.44	0	0	**191 (63.6–417)**
JUN vs. WRA	$\Theta_1, \Theta_2, \Theta_A, m_1 = m_2 = 0$	0.610	28.6	0.814	0	0	51.0 (3.0–315)
WRA vs. KET	$\Theta_1, \Theta_2, \Theta_A, m_1 = m_2 = 0$	256	642	1.26	0	0	54.3 (1.3–187)
KET vs. RUP	$\Theta_1, \Theta_2, \Theta_A, m_1 = m_2 = 0$	>250	>250	1.09	0	0	13.7 (0.2–53.4)
RUP vs. SJB	$\Theta_1 = \Theta_2 = \Theta_A, m_1, m_2 = 0$	1.090	1.090	1.090	3.6	0	13.5 (0.2–38.3)
SJB vs. CAM	$\Theta_1, \Theta_2, \Theta_A, m_1 = m_2 = 0$	0.565	0.484	1.082	0	0.2	14.8 (1.1–47.6)
CAM vs. SJI	$\Theta_1, \Theta_2, \Theta_A, m_1, m_2 = 0$	0.691	2.210	1.734	0.9	0	**106 (97.0–112)**
SJB vs. BAM	$\Theta_1, \Theta_2, \Theta_A, m_1 = m_2 = 0$	0.616	0.478	1.043	0	0	**98.0 (35.9–213)**
BAM vs. SJI	$\Theta_1, \Theta_2, \Theta_A, m_1, m_2 = 0$	0.040	1.013	2.012	0.1	0	1.2 (0–104)
Patiria miniata							
VC vs. DUN	$\Theta_1 = \Theta_2 = \Theta_A, m_1, m_2 = 0$	3.58	3.58	3.58	5.33	0	25.8 (10.3–41.6)
DUN vs. WIN	$\Theta_1 = \Theta_2 = \Theta_A, m_1, m_2$	6.90	6.90	6.90	0.004	1.68	**282 (77.5–?)**
WIN vs. AP	$\Theta_1 = \Theta_2 = \Theta_A, m_1, m_2$	7.80	7.80	7.80	0.750	0.050	**105 (63–155)**
Balanus glandula							
COR vs. SIT	$\Theta_1, \Theta_2, \Theta_A, m_1 = m_2 = 0$	64.4	52.3	12.9	0	0	**147 (77.0–265)**
SIT vs. JUN	$\Theta_1, \Theta_2, \Theta_A, m_1 = m_2 = 0$	96.2	151	6.77	0	0	**125 (49–212)**
JUN vs. RUP	$\Theta_1, \Theta_2, \Theta_A, m_1 = m_2$	18.1	16.0	1.78	30.3	30.3	**233 (102–369)**
RUP vs. REN	$\Theta_1, \Theta_2, \Theta_A, m_1 = m_2 = 0$	57.9	845	7.18	0	0	**331 (209–461)**
REN vs. SJI	$\Theta_1, \Theta_2, \Theta_A, m_1 = m_2$	168.7	634.6	6.91	49.1	49.1	**282 (168–434)**
X. mucosus							
SIT vs. SJI	$\Theta_1, \Theta_2, \Theta_A, m_1 = m_2$	0.296	0.365	0.237	1.21	1.21	0 (0–37.3)
X. atropurpureus							
SIT vs. HG	$\Theta_1 = \Theta_2 = \Theta_A, m_1, m_2$	3.16	3.16	3.16	0.165	0.165	**238 (21.2–?)**
HG vs. CAM	$\Theta_1, \Theta_2, \Theta_A, m_1, m_2 = 0$	7.31	2.75	1.53	2.02	0	**622 (323–?)**
CAM vs. SJI	$\Theta_1 = \Theta_2 = \Theta_A, m_1, m_2$	2.25	2.25	2.25	0.743	0.743	**239 (39.3–?)**

Discussion

Classification of species' histories

Based on the results from demographic analyses, we classified each species as exhibiting a recent biogeographic history consistent with either LGM persistence or post-LGM recolonization (Table 6). For most species, congruent results across analyses pointed to the same inferred history. For example, drift-mutation equilibrium statistics, mismatch analysis, and Bayesian demographic reconstructions for *E. troschelii* all yielded results consistent with a recent and large population expansion (more than a 10 fold increase in N_e) in the temporal vicinity of the LGM, whereas for *M. californianus*, results from all analyses indicated a demographic history lacking similarly consistent and clear evidence of a large demographic expansion that would be expected with a post-LGM recolonization history (Figs 2 and 6). For *M. californianus*, even though the expansion and constant size models both received strong support over the BSP (Table 4), the relatively modest change in N_e over the last 20 kyr in the expansion reconstruction (Fig. 7), combined with the weight of evidence across all other analyses, led us to favour LGM persistence for this species. A recent multilocus population genetic study also arrived at a similar conclusion, that *M. californianus* shows no evidence of a large post-LGM population expansion (Addison *et al.* 2008).

Four other species, *M. trossulus, S. cariosus, B. glandula*, and *K. tunicata,* all showed results consistent with LGM persistence. Additional analyses of these species (e.g. mtDNA divergence times between adjacent populations) were also consistent with LGM persistence (not shown). Demographic reconstructions based on nuclear EF1 sequences (Fig. 7) and multilocus population divergence times also supported LGM persistence for *B. glandula*, the same conclusion from an earlier study of mtDNA that included only sites at Bamfield, the San Juan Islands, and Juneau (Wares & Cunningham 2005). In sharp contrast, both *L. sitkana* and *X. mucosus* were easily categorized as exhibiting patterns of variation consistent with post-LGM recolonization and expansion given a near absence of mtDNA diversity; two nuclear genes also supported a history of post-LGM recolonization for *X. mucosus* (Table 3, also see Hickerson & Cunningham 2005). Although the lower bound on the confidence interval for the start of a population expansion for *P. ochraceus* (from the mismatch analysis) did not quite overlap with the LGM (Fig. 5), the modal number of differences among haplotypes was zero (Fig. 4) and the BSP for this species yielded a pattern highly consistent with a large (~50 fold) post-LGM population expansion (Fig. 7).

Significant population structure over large spatial scales in itself suggests long-term regional persistence, so not surprisingly, among four species that showed significant population genetic structure, two (*P. miniata,* & *X. atropurpureus*) yielded evidence from both mtDNA (Fig. 6) and multilocus data (Table 5) supporting long-term demographic stability and LGM persistence. The gastropod *N. lamellosa* showed both highly variable population expansion start times (Fig. 6) and interpopulation divergence times, with only the northernmost locality exhibiting clear evidence of a post-LGM expan-

Table 6 Ecological attributes, life history features, and demographic histories inferred from population genetic analyses for 14 rocky shore species

Species	Trophic Mode*	Shore position*	Development†	Coast	Inferred History
Mytilus trossulus	suspension	mid to subtidal	planktonic	both	persistence
M. californianus	suspension	mid to subtidal	planktonic	outer	persistence
Balanus glandula	suspension	mid to high	planktonic	both	persistence
Semibalanus cariosus	suspension	mid to subtidal	planktonic	both	persistence
Pisaster ochraceus	predator	mid to subtidal	planktonic	outer	recolonization
Evasterias troschelii	predator	low	planktonic	inner	recolonization
Patiria miniata	scavenger	low to subtidal	planktonic	outer	persistence
Nucella ostrina	predator	mid	benthic	outer	spatially variable
N. lamellosa	predator	low to subtidal	benthic	both	spatially variable
Katharina tunicata	grazer	mid to subtidal	planktonic	both	persistence
Littorina sitkana	grazer	mid to high	benthic	both	recolonization
L. scutulata	grazer	mid to high	planktonic	both	recolonization
Xiphister mucosus	omnivore	mid to subtidal	benthic	outer	recolonization
X. atropurpureus	omnivore	mid to subtidal	benthic	both	persistence

*Data from O'Clair & O'Clair (1998); †Data from Strathmann (1989).

sion. Private and highly divergent haplotypes were found at several localities for *N. lamellosa* (also see Marko 2004), a pattern consistent with the persistence of multiple high latitude refugia, and although most of the MLEs for population divergence times exceeded the LGM (Table 5), the confidence intervals for these estimates were very large, most overlapping with the LGM. We therefore categorized *N. lamellosa* as having a spatially variable or potentially unresolved demographic history. For *N. ostrina*, although three of four population expansion start times do not overlap with the LGM (Fig. 6), the mismatch analysis for most of the samples across southeast Alaska was consistent with a post-LGM expansion (Fig. 6). Nevertheless, the highly variable results for *N. ostrina* also indicated to us that, like *N. lamellosa*, *N. ostrina* potentially shows a more complicated pattern suggestive of a spatially variable glacial history in the northern half of its geographic range, potentially reflecting the persistence of these two species in several isolated northern refugia.

The gastropod *L. scutulata*, showed the greatest inconsistencies among analyses. Although most individuals possessed the same haplotype, the mtDNA mismatch distribution for this species was weakly bimodal, similar to *P. ochraceus*, but in contrast to *P. ochraceus*, BF tests provided support for a model of constant population size for *L. scutulata* over the last 300 kyr (Fig. 7). Even after excluding the divergent Clade 1, the preferred demographic model for *L. scutulata* in BF tests was the constant size model. However, given the relatively short history of coalescence in the BSP for Clade 2, we believe the unexpected results from the Bayesian demographic reconstructions for *L. scutulata* reflect a lack of information in the data about the rate of haplotype coalescence. Therefore, for several of the low-diversity data sets we have considered (i.e. *L. sitkana*, *X. mucosus*, & *L. scutulata*), the sudden expansion model implemented in mismatch analyses may provide a more accurate model with which to reconstruct these species recent demographic histories. Until more data demonstrate otherwise, we have classified *L. scutulata* as having undergone a recent demographic expansion, likely the result of post-LGM recolonization.

LGM community response on northeast Pacific rocky shores

Given the classifications above, our population genetic analyses of 14 ecologically prominent, co-distributed, and interacting species were not consistent with the expectation that most species have only recently recolonized the northeastern Pacific. Although patterns of mtDNA diversity, mtDNA mismatch analyses, and Bayesian demographic reconstructions for some taxa (such as the prickleback *X. mucosus*, the gastropod *L. sitkana*, and the sea stars *P. ochraceus* and *E. troschelii*) showed large post-LGM demographic expansions that would be expected as a consequence of recent recolonization from southern refugia, just as many species (such as *B. glandula*, *M. trossulus*, *M. californianus*, and *K. tunicata*) show inferred demographic histories lacking obvious signatures of massive post-LGM expansion and recolonization (Table 6). Our results contrast with those on land in this region, where mtDNA and fossil data are typically interpreted as showing patterns consistent with large post-LGM population expansions (e.g. Cwynar & MacDonald 1987; Conroy & Cook 2000; Clarke *et al.* 2001; Dembolski & Cook 2001; Nielson *et al.* 2001).

Although all 14 species showed some evidence of demographic expansions at some point in the past, the most striking result that emerged from our study is the apparent long-term demographic stability in several species over the last 150 kyr, a period of time roughly spanning the end of the glacial Illinois/Riss Stage, followed by the maximum of the relatively warm Sangamon/Riss-Würm interglacial (~120 kyrbp), the relatively cold Wisconsin/Würm glacial maximum (~20 kyrbp), returning again to the relatively warm interglacial conditions of today (Gates 1993; and references within). Although several earlier studies (Wares & Cunningham 2001, 2005; Marko 2004; Hickerson & Cunningham 2005) similarly concluded that patterns of genetic diversity in some northeastern Pacific rocky-shore species were not consistent with post-LGM recolonization, our wider survey of 14 species, combined with increased sampling of the northern half of species' ranges, indicated that LGM persistence may be a common biogeographic history among members of this community. Pre-LGM population expansions inferred from Bayesian reconstructions of demographic histories have also been reported from coastal marine species in the northeastern Atlantic (Provan *et al.* 2005; Jolly *et al.* 2006; Hoarau *et al.* 2007; Derycke *et al.* 2008), indicating that events pre-dating the LGM have been more important in shaping the demographic histories of rocky-shore species elsewhere.

There are three important caveats to these conclusions. First, the diversity of demographic histories that we have reported could reflect the stochastic and highly variable nature of patterns of coalescence among single gene genealogies. Coalescent theory, as well as some multilocus empirical studies, clearly demonstrates that population genetic inferences from single loci can be misleading (for recent reviews see Edwards & Beerli 2000; Arbogast *et al.* 2002; Brumfield *et al.* 2003). Therefore, population genetic inferences based only on mtDNA must always be treated with some caution (Ba-

zin *et al.* 2006) given that the variability of demographic histories apparent in our results (e.g. Fig. 7) could reflect, to some degree, the high variability of the coalescent. However, analyses of multilocus data for five species were consistent with the basic pattern found with mtDNA: three of those species (*B. glandula*, *P. miniata*, & *X. atropurpureus*) showed interpopulation divergence times that are significantly and uniformly older than the LGM (Table 5). The Bayesian demographic reconstruction for *B. glandula* based on nuclear EF1 also showed no evidence of post-LGM recolonization, although the large discrepancy in Φ_{ST} between COI and EF1 and the potential role of selection is noted, which will be the focus of a forthcoming paper.

Uncertainty in mutation rates is a second important caveat to our primary conclusion that regional persistence was as common a history as post-LGM recolonization. Although numerous mtDNA divergence rate estimates at the phylum and class level are available for all of the taxa we considered, we used the conservative approach of applying a relatively fast mutation rate based on a divergence rate of 2%/MY to render our conclusions conservative with respect to finding more evidence supporting LGM range expansions. Nevertheless, our conclusions about the exact timing of demographic changes could be in error if the actual mutation rates of the taxa considered here were substantially larger than our 2%/MY-based rate. Slightly faster rates have been reported for some marine taxa (e.g. Lessios *et al.* 1999; Wares & Cunningham 2001), but nearly all involved biogeographic calibrations, which tend to overestimate mutation rates (Marko 2002; Lessios 2008). Moreover, very high mutation rates would be required for several species' histories to be compatible with recent population expansions. For example, in order for the start of the population expansions in *M. californianus*, *B. glandula*, and *K. tunicata* inferred from mismatch analyses (Fig. 4) to all fall within the vicinity of the LGM, the actual mtDNA mutation rate in these taxa would have to be more than an order of magnitude greater (i.e. equivalent to an unprecedented 20%/MY divergence rate). Other species histories, such as those for *S. cariosus*, *M. trossulus*, *N. ostrina*, and *N. lamellosa*, could be potentially interpreted as compatible with the EC model if mutation rates were only two to three times greater. However, even a doubling of the mutation rate across all taxa (i.e. equivalent to a relatively large divergence rate of 4%/MY) would still leave one-third of the species' with demographic histories inconsistent with large post-LGM expansions. Therefore, we think that variation in mutation rates alone likely cannot account for the relatively deep demographic histories among many of the taxa considered here.

The third caveat to our main conclusions is that high gene flow since the LGM may have erased the signature of recent recolonization, particularly for species with planktonic larvae. In particular, the example of *L. scutulata* highlights admixture of distinct lineages as a potential confounding factor in our analyses. Admixture will upwardly bias estimates of N_e, and this bias is expected to be greatest for species with high gene flow, in which several deeply divergent haplotype lineages may have recolonized northern regions from southern refugia. Although we cannot rule out the hypothesis that gene flow following the LGM was so high that it has completely obscured all detectable traces of recent population growth, we attempted to reduce the bias of lineage admixture for species with planktonic larvae by re-analyzing individual clades with the expectation that if N_e was overestimated simply by combining distinct lineages, each individual clade should show a clearer demographic signature consistent with LGM recolonization (e.g. Wares & Cunningham 2001). Although the Bayesian demographic reconstructions do show shorter coalescent histories for some clades (e.g. Clade 2 in *S. cariosus*, Clade 2 in *M. trossulus*), the pattern of long-term stability in N_e inferred from complete data sets is largely retained in other clades within the same species (e.g. Clade 1 in *S. cariosus*, Clades 1 & 3 in *M. trossulus*), indicating that demographic histories consistent with LGM persistence in species with planktonic larvae are probably not just an artefact of lineage admixture.

Assuming the aforementioned caveats did not introduce a massive source of bias in our analyses, how can the regional persistence of taxa across glacial-interglacial climates be explained? Biophysical modelling of rocky-shore species has highlighted the fact that body temperature is not a simple function of climate, but is instead determined by a complex interaction between organism and environment, modified by local weather, shoreline position, wave exposure, and the timing of aerial exposure during low tides (Helmuth *et al.* 2002, 2006a; Gilman *et al.* 2006; Pincebourde *et al.* 2008). These models reveal the existence of a highly variable thermal mosaic of body temperatures experienced within the geographic ranges of rocky-shore species that can be more important than large-scale climate variation in determining species' distributions (Helmuth *et al.* 2006b). Although our analyses do not allow actual reconstruction of changes in species geographic ranges, the demographic histories that we have inferred for the northern ranges of 14 rocky-shore species are broadly consistent with the idea that large-scale changes in past climate did not necessarily cause simple, latitudinally-related changes in abundance and distribution across the entire community. The apparent demographic stability of some species across recent glacial-interglacial

cycles suggests some taxa may possess eurythermal physiologies, and may thus serve as significant biotic indicators for characterizing the impacts of global warming on the abundance and distributions of rocky-shore species in the northeastern Pacific.

Although heat tolerance is better characterized than cold tolerance for most intertidal taxa (e.g. Tomanek & Somero 1999; Helmuth & Hofmann 2001; Sorte & Hoffmann 2005), available cold tolerance data for the species included in our study are consistent with the histories we have inferred from genetics. Given that sea surface temperatures on the outer coast of southeast Alaska, British Columbia, and Washington dropped by ~4 °C during the last glacial (Moore *et al.* 1980; Fields *et al.* 1993), a regional decline in the keystone predator *P. ochraceus* during the last glacial is consistent with the observation that *P. ochraceus* is rendered inactive in Oregon when sea surface temperatures drop by 3–5 °C during periods of coastal upwelling of cold water to the surface (Sanford 1999). In contrast, *M. trossulus*, which showed patterns consistent with LGM demographic stability, can withstand freezing temperatures (Seed 1976; Suchanek 1978; Braby & Somero 2006). Barnacles, which also showed inferred histories of LGM stability in our study, are also legendary for their tolerance to both severe heat and cold (Southward 1964; Crisp & Ritz 1967; Cook & Lewis 1971; Wethey 2002; Berger & Emlet 2007).

Indirect effects are also potentially important (Hewitt 2004). Most notable in this regard are the contrasting histories of the keystone sea star predator *P. ochraceus* and its preferred mussel prey *M. californianus*. Experiments have shown that the absence of *P. ochraceus* on rocky shores allows the competitively dominant *M. californianus* to outcompete and exclude other low-shore and shallow subtidal macroinvertebrates and algae (Paine 1966, 1976; Menge *et al.* 1994), potentially leading to a shift to an alternative stable state in community composition due to the inability of *P. ochraceus* to successfully attack large *M. californianus* (Paine & Trimble 2004). Our analyses indicated that although *M. californianus* probably persisted in British Columbia and southeast Alaska during the LGM, our analyses also suggested *P. ochraceus* was probably effectively absent from the region. An absence of *P. ochraceus* during the LGM would be expected to cause a substantial shift in the overall community structure of the lower shore, leading to the potential competitive exclusion of other low shore species. Viewed from another perspective, however, the absence of *P. ochraceus* on the lower shore may have been an important factor in the regional persistence of *M. californianus*, allowing this competitively dominant species to exist low on the shore (and potentially subtidally, see Paine 1976) where stressful aerial exposure times are greatly reduced (Stillman & Somero 1996; Stillman 2003). This hypothesis seems plausible given that *M. californianus* is susceptible to freezing (Suchanek 1978, Suchanek 1985) and therefore could have only persisted in low-shore/subtidal habitats during glacial climates. Similarly, the recovery of *M. trossulus* populations after severe freezing events in Alaska is also strongly dependent on predation by *Nucella* (Carroll 1994; Carroll & Highsmith 1996), and the likely reduced prevalence of *N. ostrina*, *N. lamellosa* (this study), and *N. lima* (Cox & Marko unpublished) at the northern end of their current range (Fig. 6) may have similarly facilitated high latitude persistence of *M. trossulus* during the LGM.

Ecological and life history attributes

Considering only those species that show a clear history of either LGM persistence or post-LGM recolonization, the majority of species (6 of 7) with histories of LGM persistence can be found in the lowest region of the intertidal or shallow subtidal. However, if species are grouped as either inhabiting low shore habitats or not (using habitat classifications from O'Clair & O'Clair 1998), a two-tailed Fisher Exact Test applied to a 2×2 contingency table for the variables shore height (low/subtidal vs. or mid/high) and inferred biogeographic history is not significant ($P = 0.523$) because three of four expansion species also live on the low shore (Table 6). Similarly, even though most of the species for which a history consistent with persistence was inferred have planktonic larvae (6 of 7), larval developmental mode (planktonic vs. benthic) was not significantly associated with inferred history in a 2×2 contingency table ($P = 0.523$). Habitat breadth (species inhabiting both inner and outer coastal habitats vs. one or the other) also showed no significant relationship with inferred history compared to species ($P = 0.558$). Finally, even though all of the suspension feeders showed inferred histories of LGM persistence, only a marginally insignificant relationship ($P = 0.081$) was inferred from a 2×2 contingency table in which suspension feeders' histories were compared to all other feeding modes combined. Therefore, we found no strong statistical support for any single trait in explaining species' inferred histories. Nevertheless, some trends merit future consideration given that 6 of 7 (Sign Test $P = 0.0625$) species that showed clear population genetic signatures of regional persistence possess planktonic larvae and live in low shore habitats, traits that have been previously identified as important in determining species' fates during past changes in climate (Wares & Cunningham 2001; Marko 2004). Suspension feeders may also have been more likely to persist in

cooler climates (compared to benthic carnivores and herbivores), possibly due to the greater physiological costs and potential impairment of mobile lifestyles in colder climates (e.g. Sanford 1999), but the evidence for this in our analyses remains weak. We also considered diet breadth (see Hickerson & Cunningham 2005) as a potential explanatory factor, but few species in our study could be confidently classified as true diet specialists (O'Clair & O'Clair 1998). The relatively wide diets of most species and thus the lability of trophic interactions within this particular community may in fact play important roles in food web stability under changing environmental conditions (Paine 1980).

Conclusions

Unlike many mtDNA-based studies of terrestrial organisms (Hewitt 2004), our analysis of mtDNA sequences from 14 species indicates that regional persistence across the LGM is not a rare history among rocky-shore marine species of the northeast Pacific. The results suggest that the dramatic and frequent climate changes of the Pleistocene (particularly the transition from the LGM to the present interglacial), may have had less frequent community-wide impacts on the demographic and biogeographic histories of coastal marine species, at least in the northeastern Pacific. Although demographic inferences from genetic data do not reveal the actual spatial distribution of populations in the past, regional persistence over relatively long periods may have also created fewer episodes of geographic isolation caused by climate-driven fragmentation of species' ranges (e.g. Lovette 2004). Although recent genetic evidence indicates that some terrestrial species persisted in cryptic northern refugia (Stewart & Lister 2001; Provan & Bennett 2008), most of these taxa still show patterns of genetic diversity indicative of recent large population expansions (e.g. Tremblay & Schoen 1999; Abbott *et al*. 2000; Golden & Bain 2000; Anderson *et al*. 2006; Loehr *et al*. 2006). Future work investigating to what extent the apparently wide variability in demographic histories revealed in our study reflects actual demographic variation among species – vs. the variability of the coalescent – will be fundamentally important for understanding the basic question of whether co-distributed species respond to environmental change in an individualistic manner (Valentine & Jablonski 1993) or as cohesive and distinct assemblages (Fields *et al*. 1993).

Acknowledgements

The National Science Foundation (NSF OCE-0550526), the Natural Sciences and Engineering Research Council (NSERC 204-203052), Clemson University, Simon Fraser University, and the Helen Riaboff Whiteley Center provided financial support for this research. The province of British Columbia and the States of Alaska, Washington, Oregon, and California granted permission to collect specimens. We thank S. Walker, C. Neufeld, G. Pogson, S. Gilman, R. Emlet, and G. Eckert, for assistance with specimen collection. We thank S. Rogers, C. Cunningham, and two anonymous reviewers for comments and suggestions. This is Technical Contribution No. 5717 of the Clemson University Experiment Station, based upon work supported by CSREES/USDA, under project number SC-1700342. BEAST and IMa analyses were conducted on the CBSU computer clusters at the Cornell University Theory Center.

References

Abbott RJ, Smith LC, Milne RI, Crawford RMM, Wolff K, Balfour J (2000) Molecular analysis of plant migration and refugia in the Arctic. *Science*, **289**, 1343–1346.

Addicott WO (1966) Late Pleistocene marine paleoecology and zoogeography in central California. *United States Geological Survey Professional Paper*, **523-C**, 1–21.

Addison JA, Ort BS, Mesa KA, Pogson GH (2008) Range-wide genetic homogeneity in the California sea mussel (*Mytilus californianus*): a comparison of allozymes, nuclear DNA markers, and mitochondrial DNA sequences. *Molecular Ecology*, **17**, 4222–4232.

Anderson LL, Hu FS, Nelson DM, Petit RJ, Paige KN (2006) Ice-age endurance: DNA evidence of a white spruce refugium in Alaska. *Proceedings of the National Academy of Sciences U S A*, **103**, 12447–12450.

Arbogast BS, Edwards SV, Wakeley J, Beerli P, Slowinski JB (2002) Estimating divergence times from molecular data on phylogenetic and population genetic timescales. *Annual Review of Ecology and Systematics*, **33**, 707–740.

Barnes M (1989) Egg production in cirripeds. *Oceanography and Marine Biology: An Annual Review*, **27**, 91–166.

Bazin E, Glemin S, Galtier N (2006) Population size does not influence mitochondrial genetic diversity in animals. *Science*, **312**, 570–572.

Bennett KD (1997) *Evolution and Ecology: The Pace of Life*. Cambridge University Press, Cambridge.

Bennett KD, Tzedakis PC, Willis KJ (1991) Quaternary refugia of northern European trees. *Journal of Biogeography*, **18**, 103–115.

Berger MS, Emlet RB (2007) Heat-shock response of the upper intertidal barnacle *Balanus glandula*: thermal stress and acclimation. *The Biological Bulletin*, **212**, 3, 232–241.

Braby CE, Somero GN (2006) Ecological gradients and relative abundance of native (*Mytilus trossulus*) and invasive (*M. galloprovincialis*) blue mussels in the California hybrid zone. *Marine Biology*, **148**, 1249–1262.

Brumfield RT, Beerli P, Nickerson DA, Edwards SV (2003) The utility of single nucleotide polymorphisms in inferences of population history. *Trends in Ecology and Evolution*, **18**, 249–256.

Carroll ML (1994) *The Ecology of a High-Latitude Rocky Intertidal Community: Processes Driving Population Dynamics in Kachemak Bay, Alaska*. Ph.D. Thesis, University of Alaska, Fairbanks.

Carroll ML, Highsmith RC (1996) Role of catastrophic disturbance in mediating *Nucella-Mytilus* interactions in the Alaskan rocky intertidal. *Marine Ecology Progress Series*, **138**, 125–133.

Clark JS, Fastie C, Hurtt GC *et al.* (1998) Reid's paradox of rapid plant migration. *BioScience*, **48**, 13–24.

Clarke TE, Levin DB, Kavanaugh DH, Reimchem TE (2001) Rapid evolution in the *Nebria gregaria* group (Coleoptera: Carabidae) and the paleogeography of the Queen Charlotte Islands. *Evolution*, **55**, 1408–1418.

Collins TM, Frazer K, Palmer AR, Vermeij GJ, Brown WM (1996) Evolutionary history of northern hemisphere *Nucella* (Gastropoda, Muricidae): molecules, ecology, and fossils. *Evolution*, **50**, 2287–2304.

Comes HP, Kadereit JW (1998) The effect of Quaternary climatic changes on plant distribution and evolution. *Trends in Plant Science*, **3**, 432–438.

Connell JH (1970) A predator-prey system in the marine intertidal region. I. Balanus glandula and several predatory species of Thais. *Ecological Monographs*, **40**, 49–78.

Conroy CJ, Cook JA (2000) Phylogeography of a post-glacial colonizer: *Microtus longicardus* (Rodentia: Muridae). *Molecular Ecology*, **9**, 165–175.

Cook PA, Lewis AH (1971) Acquisition and loss of cold-tolerance in adult barnacles (*Balanus balanoides*) kept under laboratory conditions. *Marine Biology*, **9**, 1432–1793.

Crisp DJ, Ritz DA (1967) Changes in the temperature tolerance of *Balanus balanoides* during its life cycle. *Helgoländer wiss Meeresunters*, **15**, 98–115.

Cwynar LC, MacDonald GM (1987) Geographic variation of lodgepole pine in relation to population history. *American Naturalist*, **129**, 463–469.

Dembolski JR, Cook JA (2001) Phylogeography of the dusky shrew, *Sorex monticolus* (Insectivora: Soricidae): insight into deep and shallow history in northwestern North America. *Molecular Ecology*, **10**, 1227–1240.

Derycke S, Remerie T, Backeljau T *et al.* (2008) Phylogeography of the *Rhabditis* (*Pellioditis*) *marina* species complex: evidence for long-distance dispersal, and for range expansions and restricted gene flow in the northeast Atlantic. *Molecular Ecology*, **17**, 3306–3322.

Drummond AJ, Rambaut A (2007) BEAST: Bayesian evolutionary analysis by sampling trees. *BMC Evolutionary Biology*, **7**, 214.

Drummond AJ, Rambaut A, Shapiro B, Pybus OF (2005) Bayesian coalescent inference of past population dynamics from molecular sequences. *Molecular Biology and Evolution*, **22**, 1185–1192.

Edwards SV, Beerli P (2000) Gene divergence, population divergence, and the variance in coalescence time in phylogeographic studies. *Evolution*, **54**, 1839–1854.

Emerson BC, Hewitt GM (2005) Phylogeography. *Current Biology*, **15**, 367–371.

Excoffier L, Laval G, Schneider S (2005) ARLEQUIN (Version 3.0): an integrated software package for population genetics data analysis. *Evolutionary Bioinformatics Online*, **1**, 47–50.

Felsenstein J (1992) Estimating effective population size from samples of sequences: inefficiency of pairwise and segregating sites as compared to phylogenetic estimates. *Genetical Research*, **59**, 139–147.

Fields PA, Graham JB, Rosenblatt RH, Somero GN (1993) Effects of expected global climate change on marine faunas. *Trends in Ecology and Evolution*, **8**, 361–367.

Folmer O, Black M, Hoeh W, Lutz R, Vrijenhoek R (1994) DNA primers for amplification of mitochondrial cytochrome c oxidase subunit I from diverse metazoan invertebrates. *Molecular Marine Biology and Biotechnology*, **3**, 294–299.

Frey MA, Vermeij GJ (2008) Molecular phylogenies and historical biogeography of a circumtropical group of gastropods (Genus: *Nerita*): implications for regional diversity patterns in the marine tropics. *Molecular Phylogenetics and Evolution*, **48**, 1067–1086.

Gates DM (1993) *Climate Change and its Biological Consequences*. Sinauer Associates. Sunderland, MA.

Gilman SE, Wethey DS, Helmuth B (2006) Variation in the sensitivity of organismal body temperature to climate change over local and geographic scales. *Proceedings of the National Academy of Sciences*, **103**, 9560–9565.

Golden JL, Bain JF (2000) Phylogeographic patterns and high levels of chloroplast DNA diversity in four *Packera* (Asteraceae) species in southwestern Alberta. *International Journal of Organic Evolution*, **54**, 1566–1579.

Graham RW, Lundelius EL, Graham MA, Schroeder EK (1996) Spatial response of mammals to late quaternary environmental fluctuations. *Science*, **272**, 1601–1606.

Harley CDG, Pankey MS, Wares JP, Grosberg RK, Wonham MJ (2006) Color polymorphisms and genetic structure in the sea star *Pisaster ochraceus*. *Biological Bulletin*, **211**, 248–262.

Harpending HC (1994) Signature of ancient population growth in a low-resolution mitochondrial DNA mismatch distribution. *Human biology: An international record of research*, **66**, 4.

Hart MW, Byrne M, Smith MJ (1997) Molecular phylogenetic analysis of life-history evolution in asterinid starfish. *Evolution*, **51**, 1848–1861.

Helmuth BST, Hofmann GE (2001) Microhabitats, thermal heterogeneity, and patterns of physiological stress in the rocky intertidal zone. *Biological Bulletin*, **201**, 374–384.

Helmuth BS, Harley CDG, Halpin P, O'Donnell M, Hofmann GE, Blanchette C (2002) Climate change and latitudinal patterns of intertidal thermal stress. *Science*, **298**, 1015–1017.

Helmuth BST, Broitman BR, Blanchette CA *et al.* (2006a) Mosaic patterns of thermal stress in the rocky intertidal zone: implications for climate change. *Ecological Monographs*, **76**, 461–479.

Helmuth BST, Mieszkowska N, Moore P, Hawkins S (2006b) Living on the edge of two changing worlds: forecasting the responses of rocky intertidal ecosystems to climate change. *Annual Review of Ecology, Evolution, and Systematics*, **37**, 373–404.

Hewitt GM (1999) Post-glacial re-colonization of European biota. *Biological Journal of the Linnean Society*, **68**, 87–112.

Hewitt GM (2000) The genetic legacy of the Quaternary ice ages. *Nature*, **405**, 907–913.

Hewitt GM (2001) Speciation, hybrid zones, and Phylogeography: seeing genes in space and time. *Molecular Ecology*, **10**, 537–549.

Hewitt GM (2003) Ice ages: their impact on species distributions and evolution. In: *Evolution on Planet Earth* (eds Rothschild LJ, Lister AM), pp. 339–361, Academic Press, London.

Hewitt GM (2004) Genetic consequences of climatic oscillations in the Quaternary. *Philosophical Transactions: Biological Sciences*, **359**, 183–195.

Hewitt GM, Ibrahim KM (2001) Inferring glacial refugia and historical migrations with molecular phylogenies. In: *Integrating Ecology and Evolution in a Spatial Context. BES Symposium Volume* (ed. Silvertown J, Antonovics J), pp. 271–294. Blackwell Press, Oxford.

Hey J, Nielsen R (2004) Multilocus methods for estimating population sizes, migration rates and divergence time, with applications to the divergence of *Drosophila pseudoobscura* and *D. persimilis*. *Genetics*, **167**, 747–760.

Hey J, Nielsen R (2007) Integration within the Felsenstein equation for improved Markov chain Monte Carlo methods in population genetics. *Proceedings of the National Academy of Sciences*, **104**, 2785–2790.

Hickerson MJ, Cunningham CW (2005) Contrasting Quaternary histories in an ecologically divergent sister pair of low-dispersing intertidal fish (*Xiphister*) revealed by multilocus DNA analysis. *Evolution*, **59**, 344–360.

Hickerson MJ, Ross JRP (2001) Post-glacial population history and genetic structure of the northern clingfish (*Gobbiesox maeandricus*), revealed from mtDNA analysis. *Marine Biology*, **138**, 407–419.

Hines AH (1978) Reproduction in three species of intertidal barnacles from central California. *Biological Bulletin*, **154**, 262–281.

Hoarau G, Coyer A, Veldsink H, Stam WT, Olsen JL (2007) Glacial refugia and recolonization pathways in the brown seaweed *Fucus serratus*. *Molecular Ecology*, **16**, 3606–3616.

Hohenlohe PA (2002) Life history of Littorina scutulata and L-plena, sibling gastropod species with planktotrophic larvae. *Invertebrate Biology*, **121**, 25–37.

Hudson RR, Kaplan NL (1985) Statistical properties of the number of recombination events in the history of a sample of DNA sequences. *Genetics*, **111**, 147–164.

Huntley B, Birks HJB (1983) *An Atlas of Past and Present Pollen Maps for Europe: 0-13000 Years Ago*. Cambridge University Press, Cambridge.

Ibrahim KM, Nichols RA, Hewitt GM (1996) Spatial patterns of genetic variation generated by different forms of dispersal during range expansion. *Heredity*, **77**, 282–291.

Jeffreys H (1961) *Theory of Probability*. Oxford University Press, Oxford.

Jolly MT, Viard F, Gentil F, Thiébaut E, Jollivet D (2006) Comparative phylogeography of two coastal polychaete tubeworms in the Northeast Atlantic supports shared history and vicariant events. *Molecular Ecology*, **15**, 1840–1855.

Knowlton N, Weigt LA (1998) New dates and new rates for divergence across the Isthmus of Panama. *Proceedings of the Royal Society of London B*, **265**, 2257–2263.

Kuhner MK, Yamato J, Felsenstein J (1995) Estimating effective population size and mutation rate from sequence data using metropolis-Hastings sampling. *Genetics*, **140**, 1421–1430.

Kuhner MK, Yamato J, Felsenstein J (1998) Maximum likelihood estimation of population growth rates based on the coalescent. *Genetics*, **149**, 429–434.

Kyle CJ, Boulding EG (1998) Molecular genetic evidence for parallel evolution in a marine gastropod, Littorina subrotundata. *Proceedings of the Royal Society of London, Biological Sciences*, **265**, 1393, 303–308.

Kyle CJ, Boulding EG (2000) Comparative population genetic structure of marine gastropods (*Littorina* spp.) with and without pelagic larval dispersal. *Marine Biology*, **137**, 835–845.

Lessios HA (2008) The great American schism: divergence of marine organisms after the rise of the Central American Isthmus. *Annual Review of Ecology, Evolution, and Systematics*, **39**, 63–91.

Lessios HA, Kessing BD, Robertson DR, Paulay G (1999) Phylogeography and morphological divergence among morphotypes of the isopod Excirolana on the two sides of the Isthmus of Panama. *Evolution*, **48**, 530–548.

Lessios HA, Garrido MJ, Kessing BD (2001) Demographic history of *Diadema antillarum*, a keystone herbivore on Caribbean reefs. *Proceedings of the Royal Society of London, Biological Sciences*, **268**, 2347–2353.

Lindberg DR, Lipps JH (1996). Reading the chronicle of quaternary temperate rocky shore faunas. In: *Evolutionary Paleobiology* (eds Jablonski D, Erwin DH, Lipps JH), pp. 161–182. University of Chicago Press, Chicago.

Loehr J, Worley K, Grapputo A, Carey J, Veitch A, Coltman DW (2006) Evidence for cryptic glacial refugia from North American mountain sheep mitochondrial DNA. *Journal of Evolutionary Biology*, **19**, 419–430.

Lomolino MV, Riddle BR, Brown JH (2006) *Biogeography*, 3rd edn. Sinauer Associates, Inc., Sunderland, MA.

Lovette IJ (2004) Glacial cycles and the tempo of avian speciation. *Trends in Ecology and Evolution*, **20**, 57–59.

Marko PB (2002) Fossil calibration of molecular clocks and the divergence times of geminate species pairs separated by the Isthmus of Panama. *Molecular Biology and Evolution*, **19**, 2005–2021.

Marko PB (2004) 'What's larvae got to do with it?' Disparate patterns of post-glacial population structure in two benthic marine gastropods with identical dispersal potential. *Molecular Ecology*, **13**, 597–611.

Mastro E, Chow V, Hedgecock D (1982) *Littorina scutulata* and *Littorina plena:* sibling species status of 2 prosobranch gastropod species confirmed by electrophoresis. *Veliger*, **24**, 239–246.

Menge BA (1974) Effect of wave action and competition on brooding and reproductive effort in the sea star *Leptasterias hexactis*. *Ecology*, **55**, 84–93.

Menge BA, Branch GM (2001) Rocky intertidal communities. In: *Marine Community Ecology*, (eds Bertness MD, Gaines SD, Hay M), pp. 221–251. Sinauer Associates, Sunderland, MA.

Menge BA, Berlow EL, Blanchette CA, Navarette SA, Yamada SB (1994) The keystone species concept: variation in interaction strength in a rocky intertidal habitat. *Ecological Monographs*, **64**, 249–286.

Moore TC, Burckle LH, Geitzenauer K, Luz B (1980) The reconstruction of sea surface temperatures in the Pacific Ocean of 18,000 B.P. *Marine Micropaleontology*, **5**, 215–247.

Newton MA, Raftery AE (1994) Approximate Bayesian inference with the weighted likelihood bootstrap (with discussion). *Journal of the Royal Statistical Society, Series B*, **56**, 3–48.

Nielson M, Lohman K, Sullivan J (2001) Phylogeography of the tailed frog (*Ascaphus truei*): implications for the biogeography of the Pacific northwest. *Evolution*, **55**, 147–160.

Nimitz MA, Giese AC (1964) Histochemical changes correlated with reproductive activity and nutrition in the chiton, Katharina tunicata. *Quarterly Journal of Microscopical Science*, **105**, 481–495.

O'Clair RM, O'Clair CE (1998) *Southeast Alaska's Rocky Shores: Animals*. Plant Press, Auke Bay.

Paine RT (1966) Food web complexity and species diversity. *American Naturalist*, **100**, 65–75.

Paine RT (1976) Biological observations on a subtidal *Mytilus californianus* bed. *The Veliger*, **19**, 125–130.

Paine RT (1977) Controlled manipulations in the marine intertidal zone, and their contributions to ecological theory. In: *Changing Scenes in the Natural Sciences* (ed. Goulden CE), Academy of Natural Sciences, Philadelphia, pp. 245–270.

Paine RT (1980) Food webs: linkage, interaction strength, and community infrastructure. *Journal of Animal Ecology*, **49**, 667–685.

Paine RT (1994) *Marine Rocky Shores and Community Ecology: An Experimentalist's Perspective*. Ecology Institute, Oldendorf/Luhe, 152 p.

Paine RT, Levin S (1981) Intertidal landscapes: disturbance and the dynamics of pattern. *Ecological Monographs*, **51**, 145–178.

Paine RT, Trimble AC (2004) Abrupt community change on a rocky shore – biological mechanisms contributing to the potential formation of an alternative stable state. *Ecology Letters*, **7**, 441–445.

Pielou EC (1991) *After the ice age: The Return of Life to Glaciated North America*. University of Chicago Press, Chicago.

Pincebourde S, Sanford E, Helmuth BST (2008) Body temperature during low tide alters the feeding performance of a top intertidal predator. *Limnology and Oceanography*, **53**, 1562–1573.

Pluzhnikov A, Donnelly P (1996) Optimal sequencing strategies for surveying molecular genetic diversity. *Genetics*, **144**, 1247–1262.

Posada D, Crandall KA (1998) ModelTest: testing the model of DNA substitution. *Bioinformatics*, **14**, 817–818.

Provan J, Bennett KD (2008) Phylogeographic insights into cryptic glacial refugia. *Trends in Ecology and Evolution*, **23**, 564–571.

Provan J, Wattier RA, Maggs CA (2005) Phylogeographic analysis of the red seaweed Palmaria palmata reveals a Pleistocene marine glacial refugium in the English Channel. *Molecular Ecology*, **14**, 793–803.

Raffaelli D, Hawkins S (1999) *Intertidal Ecology*, 2nd edn. Kluwer Academic Publishers, London.

Redelings BD, Suchard MA (2005) Joint Bayesian estimation of alignment and phylogeny. *Systematic Biology*, **54**, 401–418.

Reid DG, Rumbak E, Thomas RH (1996) DNA, morphology, and fossils: phylogeny and evolutionary rates of the gastropod genus *Littorina*. *Philosophical Transactions: Biological Sciences*, **351**, 877–895.

Rogers AR, Harpending H (1992) Population growth makes waves in the distribution of pairwise genetic differences. *Molecular Biology and Evolution*, **9**, 552–569.

Rozas J, Sánchez-DelBarrio JC, Messeguer X, Rozas R (2003) DnaSP, DNA polymorphism analyses by the coalescent and other methods. *Bioinformatics*, **19**, 2496–2497.

Sanford E (1999) Regulation of keystone predation by small changes in ocean temperature. *Science*, **283**, 2095–2097.

Seed R (1976) *Ecology*. In: *Marine Mussels: Their Ecology and Physiology* (ed. Bayne BL), pp. 13–60, Cambridge University Press, Cambridge.

Sorte CJB, Hoffmann GE (2005) Thermotolerance and heat-shock protein expression in Northeastern Pacific Nucella species with different biogeographical ranges. *Marine Biology*, **146**, 985–993.

Sotka EE, Wares JP, Barth JA, Grosberg R., Palumbi SR (2004) Strong genetic clines and geographical variation in gene flow in the rocky intertidal barnacle *Balanus glandula*. *Molecular Ecology*, **13**, 2143–2156.

Southward AJ (1964) The relationship between temperature and rhythmic cirral activity in some Cirripedia considered in connection with their geographic distribution. *Helgoländer wiss Meersunters*, **10**, 391–403.

Spight TM (1975) On a snail's chances of becoming a year old. *Oikos*, **26**, 9–14.

Spight TM (1982) Population sizes of two marine snails with a changing food supply. *Journal of Experimental Marine Biology and Ecology*, **57**, 195–2127.

Stephens M, Smith N, Donnelly P (2001) A new statistical method for haplotype reconstruction from population data. American. *Journal of Human Genetics*, **68**, 978–989.

Stewart JR, Lister AM (2001) Cryptic northern refugia and the origins of the modern biota. *Trends in Ecology and Evolution*, **16**, 608–613.

Stillman JH (2003) Acclimation capacity underlies susceptibility to climate change. *Science*, **301**, 65.

Stillman JH, Somero GN (1996) Adaptation to temperature stress and aerial exposure in congeneric species of intertidal porcelain crabs (genus *Petrolisthes*): Correlation of physiology, biochemistry and morphology with vertical distribution. *Journal of Experimental Biology*, **199**, 1845–1855.

Strathmann MF (1989) *Reproduction and Development of Marine Invertebrates of the Northern Pacific Coast: Data and Methods for the Study of Eggs, Embryos, and Larvae*. University of Washington Press, Seattle.

Suchanek TH (1978) The ecology of *Mytilus edulis* L. in exposed rocky intertidal communities. *Journal of Experimental Marine Biology and Ecology*, **31**, 105–120.

Suchanek TH (1981) The role of disturbance in the evolution of life history strategies in the intertidal mussels *Mytilus edulis* and *M. californianus*. *Oecologia*, **50**, 143–152.

Suchanek TH (1985) Mussels and their role in structuring rocky shore communities. In: *The Ecology of Rocky Coasts* (eds. Moore PG, Seed R), pp. 70–96. Hodder & Stoughton, London.

Suchard MA, Weiss RE, Sinsheimer JS (2001) Bayesian selection of continuous-time Markov chain evolutionary models. *Molecular Biology and Evolution*, **18**, 1001–1013.

Swofford DL (2002) *Phylogenetic Analysis Using Parsimony (and Other Methods)* PAUP *4.0b4*. Sinauer Associates, Sunderland, Massachusetts.

Taberlet P, Fumagalli L, Wust-Saucy AG, Cosson JF (1998) Comparative phylogeography and postglacial colonization routes in Europe. *Molecular Ecology*, **7**, 453–464.

Tomanek L, Somero GN (1999) Evolutionary and acclimation-induced variation in the heat-shock responses of congeneric marine snails (genus: *Tegula*) from different thermal habitats: implications for limits of thermotolerance and biogeography. *Journal of Experimental Biology*, **202**, 2925–2936.

Tremblay NO, Schoen DJ (1999) Molecular phylogeography of *Dryas integrifolia*: glacial refugia and postglacial recolonization. *Molecular Ecology*, **8**, 1187–1198.

Valentine JW (1989) How good was the fossil record? Clues from the Californian Pleistocene *Paleobiology*, **15**, 83–94.

Valentine JW, Jablonski D (1993) Fossil communities: compositional variation at many time scales. In: *Species Diversity in Ecological Communities: Historical and Geographic Perspectives* (eds Ricklefs RE, Schluter D), pp. 341–349. University of Chicago Press, Chicago, IL.

Waples RS, Gaggiotti O (2006) What is a population? An empirical evaluation of some genetic methods for identifying the number of gene pools and their degree of connectivity *Molecular Ecology*, **15**, 1419–1439.

Wares JP, Cunningham CW (2001) Phylogeography and historical ecology of the North Atlantic intertidal. *Evolution*, **55**, 2455–2469.

Wares JP, Cunningham CW (2005) Diversification before the most recent glaciation in *Balanus glandula*. *aBiological Bulletin*, **208**, 60–68.

Webb T, Bartlein PJ (1992) Global changes during the last 3 million years: climatic controls and biotic response. *Annual Review of Ecology and Systematics*, **23**, 141–173.

Wethey DS (2002) Biogeography, competition, and microclimate: the barnacle *Cthamalus ragilis* in New England. *Integrative and Comparative Biology*, **42**, 872–880.

Williams D, Dunkerley D, DeDekker P, Kershaw P, Chappell M (1998) *Quaternary Environments*. Arnold, London.

Woerner AE, Cox MP, Hammer MF (2007) Recombination-filtered genomic datasets by information maximization. *Bioinformatics*, **23**, 1851–1853.

Research in P.B.M.'s lab uses molecular genetic approaches to address questions related to biogeography, speciation, and conservation. J.M.H. is an undergraduate student interested in population genetics and molecular evolution. S.A.E. is a research associate with interests in molecular biology and population genetics. T.M.M. is a postdoctoral researcher focused on life history evolution and population genetics of marine species. C.K. is a graduate student whose research focuses on life history evolution and its impacts on patterns of genetic diversity within and between species. L.N.C. is a graduate student interested in phylogeography, speciation, and the role of disturbance in shaping patterns of genetic diversity in rocky shore marine species.

Supporting information

Additional supporting information may be found in the online version of this article.

Table S1 List of DNA sequence collection sites new to this study, sample sizes, and previously published sequences retrieved from GenBank. All locations are in Alaska (AK), British Columbia (BC), and Washington (WA)

Please note: Wiley-Blackwell are not responsible for the content or functionality of any supporting information supplied by the authors. Any queries (other than missing material) should be directed to the corresponding author for the article.